DMD Fast Forward. Published on December 6, 2017 as DOI: 10.1124/dmd.117.078238
This article has not been copyedited and formatted. The final version may differ from this version.

TITLE PAGE

Quantitative Expression of Hepatobiliary Transporters and Functional Uptake of Substrates in Hepatic 2D Sandwich-Cultures: A Comparative Evaluation of Upcyte and Primary Human Hepatocytes

Michelle Schaefer[*)], Gaku Morinaga, Akiko Matsui, Gerhard Schänzle, D. Bischoff and Roderich D. Süssmuth

Department of Drug Discovery Sciences, Boehringer Ingelheim Pharma GmbH & Co. KG, Birkendorfer Str. 65, 88397 Biberach an der Riss, Germany (M.S., G.S., D.B.)

Department of Pharmacokinetics and Nonclinical Safety, Kobe Pharma Research Institute, Nippon Boehringer Ingelheim Co. Ltd., Kobe, Japan (G.M., A.M.)

Institut für Chemie, Technische Universität Berlin, Straße des 17. Juni 124, 10623 Berlin, Germany (R.D.S.)

**) Current: Department of Quantitative Pharmacology and Disposition, Merck KGaA, Frankfurter Str. 250, 64293 Darmstadt, Germany (M.S.)*

DMD Fast Forward. Published on December 6, 2017 as DOI: 10.1124/dmd.117.078238
This article has not been copyedited and formatted. The final version may differ from this version.

RUNNING TITLE PAGE

Running title: Functional Expression of Transporters in Upcyte Hepatocytes

Corresponding author:

Michelle Schaefer

Dept. of Quantitative Pharmacology and Disposition

Merck KGaA

Frankfurter Str. 250, 64293 Darmstadt, Germany

Tel: +49-6151-72-20076; Fax: +49-6151-72-53676

Email: Michelle.schaefer@merckgroup.com

Number of text pages: 33

Number of tables: 4

Number of figures: 4

Number of references: 55

Number of words in *Abstract*: 239

Number of words in *Introduction*: 698

Number of words in *Discussion*: 1495

DMD Fast Forward. Published on December 6, 2017 as DOI: 10.1124/dmd.117.078238
This article has not been copyedited and formatted. The final version may differ from this version.

Non standard abbreviations

ABC	ATP-binding cassette
AhR	aryl hydrocarbon receptor
BCRP	breast cancer resistance protein
BSEP	bile salt export pump
CAR	constitutive androstane receptor
CBQCA	3-(4-carboxybenzoyl)quinolone-2-carboxaldehyde
CL	clearance
DDI	drug-drug interaction
γ-GTP	γ-glutamyl transpeptidase
HPLC	high performance liquid chromatography
LC-MS/MS	liquid chromatography coupled to tandem mass spectrometry
LOQ	limit of quantification
MATE1	multidrug and toxin extrusion protein 1
MDR1	multidrug resistance protein 1
MPP^+	N-methyl-4-phenylpyridinium acetate
MRP2	multidrug resistance-associated protein 2
NTCP	Na^+-taurocholate co-transporting polypeptide
OATP	organic anion transporting polypeptide
OCT1	organic cation transporter 1

DMD Fast Forward. Published on December 6, 2017 as DOI: 10.1124/dmd.117.078238
This article has not been copyedited and formatted. The final version may differ from this version.

OSM	oncostatin M
P450	cytochrome P450
PHH	primary human hepatocytes
PK	pharmacokinetics
PXR	pregnane X receptor
QTAP	quantitative targeted absolute proteomics
REF	relative expression factor
RT-PCR	reverse transcription polymerase chain reaction
SCHH	sandwich-cultured human hepatocytes
SLC	solute carrier
SULT	sulfotransferase
TC	taurocholate
UGT	uridine 5'-diphospho-glucuronosyltransferase
UHH	upcyte human hepatocytes
W/O	without
WME	Williams` Medium E

DMD Fast Forward. Published on December 6, 2017 as DOI: 10.1124/dmd.117.078238
This article has not been copyedited and formatted. The final version may differ from this version.

ABSTRACT

Deficient functional expression of drug transporters incapacitates most hepatic cell lines as reliable tool for evaluating transporter-mediated drug-drug interactions. Recently, genetically-modified cells, referred to as upcyte hepatocytes, have emerged as an expandable, non-cancerous source of human hepatic cells. Herein, we quantified mRNA and protein levels of key hepatobiliary transporters and assessed associated uptake activity in short- and long-term cultures of upcyte human hepatocytes (UHH), in comparison to cryopreserved primary human hepatocytes (cPHH). Expression of canalicular efflux pumps, such as MDR1/*ABCB1*, MATE1/*SLC47A1* and MRP2/*ABCC2* were relatively well preserved in UHH. By contrast, long-term cultivation of UHH in 2D-sandwich-configuration (SCUHH) was required to upregulate OATP1B1/*SLCO1B1*, OATP2B1/*SLCO2B1*, NTCP/*SLC10A1* and OCT1/*SLC22A1* mRNA expression, which correlated well with respective protein abundances. However, mRNA and protein levels of sinusoidal SLC-transporters, except for NTCP and OATP2B1, remained low in SCUHH compared to sandwich-cultured cPHH (SCHH). OCT1- and NTCP-mediated uptake of MPP^+ and taurocholate was demonstrated in both hepatic models, whereas active uptake of OATP1B1/1B3-selective marker substrates, paralleled by markedly reduced *SLCO1B1/1B3* expression, were not detectable in SCUHH. Uptake studies under Na^+-depletion and excess of taurocholate confirmed the presence of functional NTCP protein and indicated that NTCP, apart from OATP2B1, contributed substantially to the overall hepatic uptake of rosuvastatin in SCUHH. In conclusion, our data suggest that SCUHH, despite their limitation for evaluating OATP1B1/1B3-mediated transport processes, retain NTCP-, OATP2B1- and OCT1-transport activities and thus may be considered as tool for elucidating compensatory uptake pathways for OATP1B1/1B3 substrates.

DMD Fast Forward. Published on December 6, 2017 as DOI: 10.1124/dmd.117.078238
This article has not been copyedited and formatted. The final version may differ from this version.

INTRODUCTION

Pharmacokinetics (PK) and target tissue exposure of xenobiotics are determined actively by basolateral uptake and efflux processes, metabolism as well as by biliary and renal excretion. Major involvement of hepatic transporters in the net hepatic clearance (CL) of a drug also implies susceptibility for drug-drug interactions (DDIs) and the risk for undesired side-effects (Liu and Sahi, 2016). Thus, regulatory agencies advise to critically evaluate the likelihood of an interaction between investigational new molecular entities (NMEs) and drug transporters during early drug development (Patel et al., 2016).

The use of fresh or cryopreserved primary human hepatocytes (cPHH) as holistic preclinical model is clearly the most appropriate choice for studying hepatobiliary clearance of NMEs (Menochet et al., 2012; Yoshida et al., 2013). Despite being commercially available, the broad phenotypic variability in cytochrome P450 (P450)/UDP-glucuronosyltransferase (UGT) and/or drug transporter expression and activity often requires a costly and time-consuming pre-characterization of different hepatocyte batches. Ultimately, the ones identified as appropriate will be limited in the number of cells available. Against this backdrop, in vitro models building on proliferating hepatic cells of human cancerous or non-cancerous origin, provided that hepatic physiology is well reflected, would certainly be of interest for DMPK screening cascades. In this respect, differentiated HepaRG cells have been proposed as surrogate for cPHH. In contrast to other hepatoma cell lines like HepG2 or Huh-7 (Le Vee et al., 2006; Guo et al., 2011; Juoan et al., 2016), mRNA and protein expression of important transporters of the solute carrier (SLC) and ATP-binding cassette (ABC) family, as well as associated uptake of typical marker substrates, has been demonstrated for the HepaRG cell line (Le Vee et al., 2013; Kotani et al., 2012). Certainly, particular consideration must be

given to the fact that HepaRG cells, as a mixed population of hepatocyte-like and biliary epithelial-like cells (Aninat et al., 2006), only represent the phenotype of one single donor.

A method including transduction of lentiviral constructs carrying human papilloma virus oncogenes has been described recently (Levy et al., 2015), by which the proliferative capability of PHH can be transiently induced via oncostatin M (OSM). This novel upcyte technique, theoretically applicable to any desired hepatocyte donor, led to the introduction of second-generation cryopreserved upcyte human hepatocytes (UHH), available at a virtually unlimited quantity per donor. Unlike HepG2, differentiated UHH exhibit key attributes of mature hepatic cells, including functional AhR- (aryl hydrocarbon receptor), CAR- (constitutive androstane receptor) and PXR- (pregnane X receptor) mediated P450 regulation (Ramachandran et al., 2015), functional epithelial polarization and bile flow (Levy et al., 2015), ureogenesis, and albumin synthesis (Tolosa et al., 2016), supporting their usefulness as screening in vitro tool for DDI and hepatotoxicity assessment (Ramachandran et al., 2015; Tolosa et al., 2016). In addition, we reported recently on the P450-, UGT- and sulfotransferase (SULT)-mediated metabolic capability of cultured UHH and demonstrated their utility as hepatic model for intrinsic clearance determinations of slowly metabolized drugs (Schaefer et al., 2016). Despite this broad characterization of UHH, only limited data on the expression of drug transporters, in particular for clinically relevant hepatic transporters including organic anion transporting polypeptide 1B1/1B3 (OATP1B1/1B3 encoded by *SLCO1B1/1B3*) are currently available. Compared to HepG2 cells, considerably higher mRNA expression of Na^+-taurocholate co-transporting polypeptide (NTCP/*SLC10A1*) was observed in differentiated UHH (Tolosa et al., 2016), coinciding with the report by Levy et al. (2015) for NTCP, organic cation transporter 1 (OCT1/*SLC22A1*), multidrug resistance protein 1 (MDR1/*ABCB1*) and bile salt export pump (BSEP/*ABCB11*). Although these results

indicate the preservation of selected uptake and efflux transporters in UHH, data on functional activity has not yet been reported.

The present study was designed to address questions regarding the applicability of UHH for xenobiotic-transport studies and their potential use for evaluating synergistic intrinsic CL processes. To this end, we analyzed the expression of PK- and DDI-relevant sinusoidal uptake and canalicular efflux transporters using plated UHH derived from three different donors in conjunction with cultivation-duration, and finally assessed associated uptake activity of OATPs, NTCP and OCT1. cPHH from three donors served as reference. To our knowledge, this is the first comprehensive report describing the abundance of drug transporters in long-term sandwich-cultures of UHH at the gene, protein and functional levels, compared to sandwich-cultured human hepatocytes (SCHH).

DMD Fast Forward. Published on December 6, 2017 as DOI: 10.1124/dmd.117.078238
This article has not been copyedited and formatted. The final version may differ from this version.

MATERIALS AND METHODS

Chemicals and Reagents. Calcium chloride, choline chloride, D-glucose solution (10%), dexamethasone, dimethylsulfoxide, estradiol-17ß-glucuronide ($E_2$17ßG), HEPES solution, hydrochloric acid solution (1N, cell-culture tested), magnesium sulfate, N-methyl-4-phenylpyridinium acetate (MPP^+), penicillin-streptomycin (100x), potassium bicarbonate, potassium chloride solution (75 mM), potassium phosphate monobasic, pravastatin, rifamycin SV sodium salt, sodium chloride, sodium bicarbonate solution (7.5%), sodium hydroxide solution (NaOH, 1N, cell-culture tested), sodium phosphate dibasic, sodium phosphate monobasic, sodium taurocholate, trypan blue solution and Williams´ Medium E (WME) were purchased from Sigma-Aldrich (St. Louis, MO, USA). Cholecystokinin-8 (CCK-8) was obtained from Bachem (Bubendorf, Switzerland), rosuvastatin from American Radiolabeled Chemicals (St. Louis, MO, USA). Cryopreserved hepatocyte recovery medium (CHRM), HEPES buffer (1M, pH 7.4), Fetal bovine serum (FBS), Dulbecco´s phosphate buffered saline (D-PBS) with (w/) and without (w/o) calcium or magnesium, and stabilized L-glutamine (Glutamax™, 100x) was from Life Technologies (Darmstadt, Germany), high viability cryohepatocyte recovery medium, insulin-transferrin-selenous acid and bovine serum albumin pre-mix (ITS^+, 100x), Matrigel™ phenolred-free from Corning/BD Biosciences (Bedford, MA, USA) and trypsin/ETDA (0.5/0.2%) from PAN Biotech (Aidenbach, Germany). Hepatocyte Thawing Medium (HTM), Hepatocyte Culture Medium (HCM), Hepatocyte High Performance Medium (HPM) and supplemental reagents B and C were purchased from upcyte technologies GmbH (Hamburg, Germany). [^{3}H]taurocholic acid (9.7 Ci/mmol) and [^{3}H]N-methyl-4-phenylpyridinium acetate (80 Ci/mmol) were purchased from PerkinElmer (Boston, MA, USA), [^{3}H]rosuvastatin (10 or 20 Ci/mmol), [^{3}H]pravastatin (5 Ci/mmol), [^{3}H]estradiol-17ß-glucuronide (50 Ci/mmol) and [^{3}H]cholecystokinin octapeptide (98.7

DMD Fast Forward. Published on December 6, 2017 as DOI: 10.1124/dmd.117.078238
This article has not been copyedited and formatted. The final version may differ from this version.

Ci/mmol) were obtained from American Radiolabeled Chemicals (St. Louis, MO, USA). All peptides and stable isotope-labeled (SIL) peptides were purchased from Proteomedix Frontiers Inc. (Sendai, Japan).

Short-term and 2D Sandwich-Culture of Upcyte Hepatocytes. Upcyte human hepatocytes (UHH) from female Caucasian donors (151-03, 653-03, 10-03) were purchased from upcyte technologies GmbH (Hamburg, Germany) at a population doubling (PD) range of 25-30. Thawing and culturing of cryopreserved UHH was performed as described previously (Schaefer et al., 2016). Briefly, after rapid thawing at 37°C, cells were suspended in 50 mL HTM and sedimented at 90 *g* for 5 minutes at RT. Viability and cell number, as determined by trypan blue exclusion, were highly consistent among donor batches. Seeding onto collagen I-coated T-150 flasks (Corning/BD Biosciences, Bedford, MA, USA) was performed at 5-6 x 10^3 cells/cm² in HCM supplemented with 100 U/mL penicillin, 100 µg/mL streptomycin, 2 mM L-glutamine, dimethylsulfoxide (0.5%), and reagents B and C as part of the vendor´s proprietary culture media kit. UHH cultures were passaged after 5 days of culture at 95% humidity, 37°C, 5% CO_2 with fresh medium supplied every 48 hrs and further expanded for additional 2 days in collagen I-coated T-150 flasks at 5-6 x 10^3 cells/cm². Final plating after expansion was done onto collagen I-coated 24-well plates (Corning/BD Biosciences, Bedford, MA, USA) at a density of 1.5 x 10^5 cells/cm². Short-term cultures were assessed 4-6 hrs after seeding; whereas Matrigel™ overlay at 0.125 mg/well in HPM (supplemented with 100 U/mL penicillin, 100 µg/mL streptomycin, 2 mM L-glutamine, dimethylsulfoxide (0.1%), and reagent A) was applied 4-6 hrs after seeding for long-term sandwich cultures (SCUHH). SCUHH were maintained for up to 14 days with daily media change. Morphological integrity

DMD Fast Forward. Published on December 6, 2017 as DOI: 10.1124/dmd.117.078238
This article has not been copyedited and formatted. The final version may differ from this version.

and confluence was confirmed by light microscopy (Eclipse TS100, Nikon GmbH, Düsseldorf, Germany) prior to experiments.

Primary Human Hepatocyte Cultures. Cryopreserved PHH (cPHH) from one male (Hu1601) and three female (371, HC3-31, HC3-26) Caucasian donors (Supplemental Table 1) were purchased from Life Technologies GmbH (Darmstadt, Germany), Corning/BD Gentest (Bedford, MA, USA) and TebuBio GmbH (Offenbach, Germany), respectively. Cells were thawed using the vendor's recovery medium (CHRM medium, Life Technologies GmbH, Darmstadt, Germany; high viability cryohepatocyte medium, Corning/BD Gentest, Bedford, MA, USA), sedimented for 10 minutes at 100 *g* at room temperature and finally plated onto collagen-I-coated 24-well plates (APSciences, Inc. Columbia, MD, USA) at cell densities of 375,000 or 400,000 viable cells per well in Williams' Medium E (WME) supplemented with 5% fetal bovine serum, 15 mM HEPES (pH 7.4), 6.25 µg/mL insulin, 6.25 µg/mL transferrin, 6.25 ng/mL selenous acid, 5.35 µg/mL linoleic acid, 1.25 mg/mL bovine serum albumin, 1 µM dexamethasone, 100 U/mL penicillin, 100 µg/mL streptomycin and 2 mM L-glutamine (WME complete with 1 µM dexamethasone). Attached cPHH were overlaid 4-6 hrs after plating with 0.125 mg of Matrigel^{TM} per well in WME complete plus 0.1 µM dexamethasone and maintained for up to 7 days at 95% humidity, 37°C and 5% CO_2 with daily medium changes. Uptake assays with probe substrates, as well as isolation of total RNA and plasma membrane protein, were conducted at day 0 (4-6 hours after plating; herein referred to as short-term culture) or at day 7 (long-term sandwich-culture; SCHH). Cultures were examined by light microscopy for intact morphology and confluence prior to experiments.

DMD Fast Forward. Published on December 6, 2017 as DOI: 10.1124/dmd.117.078238
This article has not been copyedited and formatted. The final version may differ from this version.

Quantitative RT-PCR Gene Expression Analysis. Total RNA was isolated as described previously (Schaefer et al., 2016) in parallel to uptake experiments. In brief, three to four wells of cultured cells were pooled for each assay time point. The RNeasy Mini Kit protocol (Qiagen, Hilden, Germany) together with the Qiagen QIAshredder homogenization and on-column DNA digestion (RNase-free DNase Set, Qiagen, Hilden, Germany) was used for RNA isolation. Purified RNA was quantified spectrophotometrically (NanoDrop 1000 spectrophotometer; Thermo Fisher Scientific, Schwerte, Germany). Total RNA (400 ng per sample) was reverse-transcribed for first-strand cDNA synthesis following the protocol for High Capacity cDNA RT Kit (Applied Biosystems, Foster City, CA, USA). Relative mRNA expression of selected hepatic uptake (*SCLO1B1*, *SLCO1B3*, *SLCO2B1*, *SLCO10A1* and *SLC22A1*) and canalicular expressed transporters (*ABCB1*, *ABCC2*, *ABCG2*, *ABCB11* and *SLC47A1*) were analyzed by quantitative real-time PCR using inventoried TaqMan gene expression assays (Life Technologies/AB, Darmstadt, Germany; Supplemental Table 2). Threshold cycle (Ct)-values were determined using the 7500 Fast software v2.06 (Applied Biosystems, Darmstadt, Germany). The gene ß-actin served as endogenous control for normalization of gene expression data and was quantified separately on each assay plate. Cycle-threshold values of $\geqslant$36 were defined as below the limit of quantification (LOQ) and set to zero for subsequent calculations.

Plasma Membrane Protein Extraction and Enzymatic Digestion. Cultured cells (7.2-9.6 x 10^6 cells per sample) were harvested from 24-well culture plates using mini cell scraper (Biotium Inc., Fremont, CA, USA) and ice-cold phosphate-buffer saline as described previously (Schaefer et al., 2012). Cell collection and centrifugation steps were conducted in LoBind centrifugation tubes (Eppendorf, Hamburg, Germany) and cell pellets were

immediately stored at -80°C after snap-freezing in liquid nitrogen. The proteomic method applied in this study was adapted on the basis of techniques developed at Tohoku University (Sendai, Japan). Cell fractionation and separation of plasma membrane fraction were conducted by differential centrifugation as reported by Sakamoto et al. (2011), Ohtsuki et al. (2012) and Schaefer et al. (2012) with minor modifications. In brief, the combined cell pellet was lysed by sonification for 1.5 minutes at 0°C in buffer A (0.15 M KCl, 0.1 M phosphate buffer pH 7.4 and 0.5 mM of the protease inhibitor phenylmethylsulfonylfluoride (PMSF)) using a Bioruptor (Cosmo Bio, Tokyo, Japan). Homogenates were centrifuged at 10,700 *g* for 20 minutes at 4°C, post-nuclear supernatants collected and sedimented twice at 100,000 *g* for 60 minutes at 4°C. The resulting microsomal pellet was suspended in buffer B (0.25 M sucrose, 20 mM Tris-HCl, pH 7.4), layered on top of a 38% (w/v) sucrose solution and ultracentrifuged at 100,000 *g* for 40 minutes at 4°C. The turbid interface fraction was recovered, suspended in buffer B, and sedimented at 100,000 *g* for 60 minutes at 4°C. Subsequent steps have been modified from the previously published method (Schaefer et al 2012). Membrane protein solubilization was performed using the Membrane Protein Extraction (MPEX) phase-transfer surfactant (PTS) reagent kit (GL Science, Tokyo, Japan) following the assay kit protocol provided with minor modifications (Masuda et al., 2008; Masuda et al., 2009). Total protein content of enriched plasma membrane proteins was determined using the CBQCA Protein Quantitation kit (Thermo Fisher, Waltham, MA, USA). MPEX PTS reagents (containing sodium desoxycholate (DOC)) were added to 5 µg of plasma membrane to a final volume of 89 µL, incubated/denatured at 95°C for 5 minutes and solubilized by subsequent sonication for 10 minutes. Samples were reduced in the presence of 1.3 mM dithiothreitol for 30 minutes at room temperature and alkylated with 2.9 mM iodoacetamide for 30 minutes at room temperature protected from light. After addition of

DMD Fast Forward. Published on December 6, 2017 as DOI: 10.1124/dmd.117.078238
This article has not been copyedited and formatted. The final version may differ from this version.

0.05 % (w/v) of the trypsin enhancer ProteaseMax ((PMX) Promega, Madison, WI, USA), sequential proteolytic digest was performed with lysyl endopeptidase ((LysC), Wako, Osaka, Japan) for 3 hrs at room temperature at an enzyme/protein ratio of 1:100, followed by in-solution digestion with sequencing grade, TPCK (L-/tosylamido-2-phenyl)ethylchloromethyl ketone)-treated trypsin (Promega, Madison, WI, USA) for 16 hrs at 37°C (ratio 1:100) in a final volume of 100 µL. Digested samples were spiked with stable-isotope labeled (SIL) peptides (Proteomedix Frontiers Inc., Sendai, Japan) as internal standards prior to liquid-liquid-extraction. An equal volume of ethyl acetate was added, samples acidified with 1% trifluoroacetic acid followed by vortexing and centrifugation. The peptide-containing aqueous phase was recovered, desalted using GL-Tips GC (GL Sciences, Tokyo, Japan) and the dried residue dissolved in 0.1 % formic acid.

Surrogate Peptide Selection. Proteotypic signature peptides for quantification of target proteins were designed and chemically synthesized based on an established *in silico* method and reported selection criteria (Tohoku University algorithm, Sendai, Japan; Kamiie et al., 2008; Uchida et al., 2013). Target peptides selected herein have been used previously by our laboratory or by others (Supplemental Table 3; Sakamoto et al., 2011; Uchida et al., 2011; Ohtsuki et al., 2012; Schaefer et al., 2012; Kunze et al., 2014), respectively, except of peptide probes for OATP1B1 and OATP2B1 (Table 1). Although originally designed in avoidance of transmembrane regions, it has become apparent that previous peptides (OATP1B1_peptide A, OATP2B1_peptide A) contain or overlap with transmembrane topological domains of target proteins, respectively, according to updated information and recent protein database searches (Supplemental Figure 1). Thus, previous peptides do no longer comply with our selection criteria initially specified. Alternative proteotypic peptide probes for OATP1B1 and

DMD Fast Forward. Published on December 6, 2017 as DOI: 10.1124/dmd.117.078238
This article has not been copyedited and formatted. The final version may differ from this version.

OATP2B1 (OATP1B1_peptide B and OATP2B1_peptide B; Table 1) have been designed, synthesized and analyzed by Proteomedix Frontiers Inc. (Sendai, Japan) to meet the reported criteria (Kamiie et al., 2008; Uchida et al., 2013; Supplemental Figure 1). Selected ions and MRM transitions for the quantification of transporter peptides have been reported previously (Sakamoto et al., 2011; Uchida et al., 2011; Supplemental Table 3); SRM/MRM conditions for OATP1B1 and OATP2B1 peptides were optimized and defined as described by Sakamoto et al. (2011).

Multiplexed-MRM Analysis using LC-MS/MS. Surrogate peptides released by tryptic digest from ten selected target drug transporters, Na^+/K^+-ATPase and γ-glutamyl transpeptidase (γ-GTP) were simultaneously detected by multiplexed selected/multiple reaction monitoring (SRM/MRM) analysis using corresponding SIL-peptides as internal standards (IS) for target peak recognition and normalization as described previously (Sakamoto et al. 2011). In brief, a 5500 QTRAP (AB Sciex, Foster City, CA, USA) electrospray ionization mass spectrometer coupled to an Ultimate 3000 (Dyonex, Amsterdam, The Netherlands) nano-LC system consisting of a loading column (L-Column2 ODS, 5 µm particle size, 300 µm inner diameter, 5 mm length from CERI, Tokyo, Japan or ACQUITY UPLC M-Class HSS T3, 5 µm particle size, 300 µm inner diameter, 50 mm length from Waters, Milford, MA, USA) and an analytical C18 nano-LC column (L-Column2 ODS, 3 µm particle size, 100 µm inner diameter, 150 mm length from CERI, Tokyo, Japan) was used for sample analysis. Mobile phases consisted of aqueous formic acid (0.1 %; A) and aqueous acetonitrile (95 % with 0.1 % formic acid; B). Purified samples (30 µL/sample i.e. 0.75 µg protein/sample) were separated and eluted from the analytical column at RT applying a linear gradient from 0-50% of eluent B at a flow rate on 200 nL/min with a run time of 60 minutes.

DMD Fast Forward. Published on December 6, 2017 as DOI: 10.1124/dmd.117.078238
This article has not been copyedited and formatted. The final version may differ from this version.

The gradient was further increased to 80% B in 10 minutes, then decreased to the initial gradient of 0% B with 0.1 minutes and held at 0%B for 20 minutes. For data acquisition (0-70 minutes), the mass analyzer was operated in positive ionization mode and set to multiple reaction monitoring (MRM) with four precursor/product ion transitions (Q1/Q3-1, Q1/Q3-2, Q1/Q3-3, Q1/Q3-4) monitored per target peptide and SIL internal standard (10 ms dwell time per channel), respectively. Optimized parameters for SRM/MRM analysis (four tuned transitions, declustering potential and collision energy) of target peptides have been applied as published previously (Sakamoto et al., 2011; Uchida et al., 2011; Supplemental Table 3). In case of OATP1B1 and OATP2B1 corresponding parameters are depicted in Table 1. The spray voltage was set to 2.6 kV, the entrance potential and the collision exit potential to 10 V for all conditions. Na^+/K^+-ATPase and γ-glutamyl transpeptidase (γ-GTP) were used as plasma membrane marker proteins to assess preparation quality of plasma membrane fractions between different samples of SCUHH and SCHH, respectively (Ohtsuki et al., 2012).

Calibration standards and quality control samples of mixed unlabeled peptides were prepared separately in aqueous formic acid (0.1%) by serial dilution of a stock solution (10 *f*mol/µL) as described (Sakamoto et al., 2011) for accurate bioanalytical quantification. Each calibration curve contained a zero sample and seven nonzero samples ranging from 1 to 100 *f*mol, spiked with a mixture of corresponding IS (20 *f*mol/IS); the lowest standard was run in duplicates. Quality control samples (QCs) were prepared in triplicates for each concentration at 2.5, 15 and 60 *f*mol. Ion count chromatograms were processed using Analyst MultiQuant software version 3.0 (AB Sciex, Foster City, CA, USA). Each target peptide level was quantified based on sample peaks identified at the same retention time as the corresponding SIL peptides and calibration curves were generated for every transition. Concentrations were calculated as the mean of quantitative values derived from three or four

DMD Fast Forward. Published on December 6, 2017 as DOI: 10.1124/dmd.117.078238
This article has not been copyedited and formatted. The final version may differ from this version.

out of four MRM transitions. In case fewer than three signal peaks were detectable, the mean concentration was not calculated and the abundance of peptide defined as not quantifiable (NQ), according to the methods applied in this study. In case concentrations were found below 1 *f*mol/µg protein and the corresponding peak area of detected signals of at least two MRM transitions were below 5000 counts, the limit of quantification (LOQ) was defined as described by Uchida et al. (2011). In brief, the protein level of a signature peptide equivalent to a peak area of 5000 counts was calculated based on the linear regression equations obtained from calibrations curves (determination coefficient $r^2 > 0.99$, Supplemental Table 3). Intra-assay precision and accuracy of quantification were evaluated based on the low, middle and high amount quality control samples, as described previously (Sakamoto et al., 2011).

Determination of Sinusoidal Uptake Activities in Plated Primary Human and Upcyte Human Hepatocytes. Cellular accumulation of reference compounds [^{3}H]rosuvastatin (1µM, 0.5 µCi/mL), [^{3}H]pravastatin (1µM, 0.5 µCi/mL), [^{3}H]MPP$^+$ (5 µM, 0.5 µCi/mL), [^{3}H]taurocholate (5 µM, 0.5 µCi/mL) [^{3}H]$E_2$17ßG (1µM, 0.5 µCi/mL) and [^{3}H]CCK-8 (1µM, 0.5 µCi/mL) was determined using either conventional monolayer short-term cultures (4-6 hrs after plating at high cell density) or long-term cultures in a 2D-sandwich-configuration. At designated culture time points, cell layers were rinsed twice and then pre-incubated with freshly prepared transport buffer solution I (1.8 mM $CaCl_2$, 1 mM $MgSO_4$, 5.36 mM KCl, 0.41 mM NaH_2PO_4, 1.19 mM Na_2HPO_4, 4.17 mM $NaHCO_3$, 128 mM NaCl, 20 mM D-glucose and 15 mM HEPES, adjusted to pH 7.2 with 1N NaOH solution) in the presence or absence of rifamycin SV (RIF SV; 100 µM) for 15 minutes at 37 °C. Parallel incubations at 4°C without inhibitor were conducted to assess passive diffusion. To start the uptake experiment 250 µL/well pre-warmed buffer solution containing a mixture of radiolabeled and

DMD Fast Forward. Published on December 6, 2017 as DOI: 10.1124/dmd.117.078238
This article has not been copyedited and formatted. The final version may differ from this version.

unlabeled compound at the defined assay concentration and radioactivity was added onto a pre-conditioned 24-well plate. An aliquot of 20 µL was drawn immediately afterwards and analyzed for the actual initial free substrate concentration. Incubations were terminated at different time points by quickly aspirating the substrate solution and washing the cells three times with 500 µL/well ice-cold transport buffer. After drying the plates for 20-30 minutes at 40 °C, cells were lysed with 250 µL/well 1N NaOH for at least 20 minutes before adding an equivalent volume of 1N HCl. A volume of 400 µL per sample was transferred into a scintillation vial (Pico Prias, Perkin Elmer, Boston, MA, USA), 5 mL of liquid scintillation fluid cocktail (Ultima Gold™, Perkin Elmer, Boston, MA, USA) was added and the radioactivity associated with the cell lysates was measured on a Tri-Carb 2900TR (Perkin Elmer Life and Analytical Sciences, Waltham, MA, USA). Total protein content of the lysate was determined using 20 µL per sample following the manufacturer´s protocol of the Pierce™ BCA protein assay kit (Pierce Biotechnology, Rockford, IL, USA). Activity of NTCP and its contribution to the uptake of rosuvastatin was determined using transport buffer II solution (1.2 mM $CaCl_2$, 1.25 mM $MgSO_4$, 4.7 mM KCl, 1.2 mM KH_2PO_4, 25 mM $NaHCO_3$, 110 mM NaCl, 15 mM D-glucose and 20 mM HEPES, adjusted to pH 7.2 with 1N NaOH solution), sodium-free transport buffer II (choline chloride and $KHCO_3$ replacing NaCl and $NaHCO_3$; 1N KOH solution used for pH adjustment), or transport buffer I containing an excess concentration of taurocholate.

Data Analysis of Uptake Studies. Within one experiment, all incubations were performed in triplicates (n=3) using confluent cultures of cPHH and UHH from the same seeding, respectively. Data are expressed as mean ± S.D., unless indicated otherwise. Intrinsic sinusoidal uptake activity was expressed either as uptake rate (V_{app}; pmol × min^{-1} × mg^{-1})

defined as the measured radioactivity associated with the cells (dpm/well) normalized to incubation time and protein amount (mg protein/well) or as apparent uptake clearance (CL_{app}; $\mu L \times min^{-1} \times mg^{-1}$), which was calculated from the measured radioactivity normalized to the incubation time and protein amount divided by the applied substrate concentration in the incubation buffer (dpm/µL). The apparent passive diffusion ($CL_{passive}$) was derived from uptake experiments conducted at 4°C, as described above, and subtracted from total hepatic uptake (CL_{uptake}) in order to determine transporter-mediated permeation processes (CL_{active}). Radioactivity data were corrected for background radioactivity attributed to nonspecific binding of substrate to culture plate surface and/or Matrigel^{TM}-overlay. Background radioactivity was determined by control incubations at 37°C or 4°C simultaneously in hepatocyte-free Matrigel^{TM}-containing wells. Inhibition of carrier-mediated uptake was expressed as percentage of control incubations without inhibitor.

Concentration dependence of uptake processes was analyzed from experiments conducted with eight concentrations by estimating kinetic parameters from the Michaelis-Menten equation (equation 1) using GraphPad Prism 7.0 software (GraphPad software Inc., San Diego, CA, USA):

$$v = \frac{V_{max} \times S}{K_m + S} \quad (1)$$

where v, S, K_m and V_{max} represent the maximum uptake rate of the substrate (pmol/min/mg protein), the substrate concentration in the buffer solution (µM), the Michaelis constant (µM) and the maximum uptake rate (pmol/min/mg protein), respectively.

Statistical Analysis. Comparison of uptake rates from incubations performed under different conditions e.g. in the presence or absence of an inhibitor, using the same hepatic in vitro

system, was analyzed using one-way analysis of variance (ANOVA) followed by Tukey's multiple comparison test. A significant difference was considered at *p*-values <0.05. In order to assess the correlation between quantified protein amounts and hepatic uptake rates a Pearson's correlation test was conducted. All statistical analyses and graphing were run using GraphPad Prism 7.0 software (GraphPad software Inc., San Diego, CA, USA).

DMD Fast Forward. Published on December 6, 2017 as DOI: 10.1124/dmd.117.078238
This article has not been copyedited and formatted. The final version may differ from this version.

RESULTS

Culture Time-Dependent Expression and Activity of Hepatic Drug Transporters. In terms of selecting appropriate conditions and pre-culture times for subsequent comparative studies between UHH and cPHH, we assessed the impact of culture duration on the expression of sinusoidal transporters essentially by measuring functional uptake activity. Cellular accumulation of rosuvastatin as an initial functional marker of OATP1B1/1B3 and NTCP activity (Fig. 1A) was determined at different times between day 0 (i.e. 4-6 hrs after seeding the cells at confluence in monolayer culture) and day 14 (long-term 2D sandwich-culture) and was supported by mRNA expression levels, concomitantly monitored via. qRT-PCR in UHH cultures (donor 151-03) from the same seeding. The mRNA expression profiles of each transporter increased after seeding and reached maximum levels between day five and day seven. Expression of each transporter decreased thereafter (an example of this is shown for *SLCO1B1*; Figure 1A). The bell-shaped expression profile of *SLCO1B1* correlated with the cultivation time-dependent uptake profile of rosuvastatin (Figure 1 A and B).

The linear uptake phase for all ensuing accumulation experiments was assessed in uptake experiments conducted for 0.5, 1, 2, 5, 10 and/or 20 minutes. For rosuvastatin, a considerable active uptake component into SCUHH was evident by comparing uptake rates from experiments conducted at low temperature (4°C, passive diffusion) and 37°C, particularly at days 5, 7 and 10 (Figure 1B). The carrier-mediated uptake was linear up to 5 minutes, considering the uptake profiles of day 5 and day 7 displaying maximum accumulation and highest expression levels (Figure 1A, Table 2). Consequently, incubation times of 5 minutes were used for all subsequent uptake experiments in SCUHH centering the evaluations on day 7 or day 14 in case of UHH from donor 653-03. Cells of this particular donor required a longer cultivation period in confluent sandwich-culture for maximal uptake

DMD Fast Forward. Published on December 6, 2017 as DOI: 10.1124/dmd.117.078238
This article has not been copyedited and formatted. The final version may differ from this version.

of rosuvastatin (data not shown). For taurocholate (TC) and *N*-methyl-4-phenylpyridinium acetate (MPP^+), a linear interval of active uptake was determined up to 5 minutes (MPP^+) and 10 minutes (TC), respectively. For the latter substrates, a more pronounced difference between the active and passive component of overall transport was observed, facilitating short incubation times of 1 minutes (Supplemental Figure 3). Active uptake kinetics of rosuvastatin (K_m and V_{max}) was then estimated applying the defined time of incubation to concentration-dependent uptake experiments at 37°C and 4°C after seven days in sandwich-culture (Figure 1C). The K_m-value obtained from cultured UHH (6.10 ± 1.49 µM) and the respective maximum initial uptake rate (27.0 ± 2.70 pmol/min/mg protein), were found within the range reported by others for rosuvastatin, determined in hepatocytes and transfected cell lines (Nezasa et al., 2003; Ho et al., 2006; Menochet et al., 2012), thereby supporting further investigation of this hepatic cell model for transporter function under the predetermined assay conditions.

Findings from initial time-course experiments, conducted in two separate UHH cultures of donor 151-03 (Figure 1A), were confirmed by subsequent studies focusing on day zero and days 7 or 14, respectively: In separate short-term monolayer cultures of three different UHH donors, i.e. 4-6 hrs after seeding the cells at confluence (day 0), mRNA expression levels as well as quantified peptides levels of transporter proteins OATP1B1, 1B3, 2B1, NTCP and OCT1 encoded by *SLCO1B1*, *SLCO1B3*, *SLCO2B1*, *SLC10A1* and *SLC22A1*, respectively, were below the LOQ both at the mRNA (Table 2) and protein level (Supplemental Table 5). Exceptions to this were OATP2B1 and OCT1, which were partially detectable in short-term cultures of UHH from two donors, albeit at very low levels. However, gene transcripts of sinusoidal transporters could be determined in long-term 2D sandwich-cultures (Table 2), suggesting a post-culture upregulation of genes encoding for OATP, NTCP

DMD Fast Forward. Published on December 6, 2017 as DOI: 10.1124/dmd.117.078238
This article has not been copyedited and formatted. The final version may differ from this version.

and OCT. Although basal OATP1B1/*SLCO1B1* expression was measureable, yet at quantitatively different levels comparing different batches of donor 151-03 (Figure 1A, Table 2), expression levels of OATP1B3/*SLCO1B3* remained below the LOQ for all long-term sandwich-cultures evaluated, independent from the batch or donor of UHH evaluated (Table 2). By contrast, expression levels of canalicular efflux transporters were not substantially different between short-term monolayer- and long-term sandwich-cultures, at least in cells from two of the three donors evaluated. As summarized in Table 2, expression of the multidrug resistance protein 1/ATP binding cassette protein B1 (MDR1/*ABCB1*), the multidrug resistance associated protein 2/ATP binding cassette protein C2 (MRP2/*ABCC2*), the breast cancer resistance protein/ATP binding cassette protein G2 (BCRP/*ABCG2*), the bile salt export pump/ATP binding cassette protein B11 (BSEP/*ABCB11*) and of the SLC transporter multidrug and toxic extrusion 1/solute carrier 47A1 (MATE1/*SLC47A1*) could be readily quantified at the gene level for all UHH donors evaluated.

Comparison between Transporter mRNA and Protein Abundance in 2D Sandwich-Cultures of UHH and cPHH. Expression levels determined in SCUHH were compared with those in cPHH from different donors (Supplemental Table 1), which were cultured in the same manner and analyzed in parallel. Relative mRNA expression levels for all sinusoidal solute carrier (SLC) transporters were found to be lower in SCUHH compared to those in SCHH (Figure 2A), with particularly marked difference observed for *SLCO1B3*/OATP1B3 (levels below LOQ). However, considerable basal expression was detected for *SLCO2B1*/OATP2B1 and *SLC10A1*/NTCP with interindividual levels of 4.7-24% and 1.6-10% of those in SCHH, respectively (Figure 2A). Among the canalicular localized drug transporters of the ATP-binding cassette (ABC) transporter family, noticeable high expression

DMD Fast Forward. Published on December 6, 2017 as DOI: 10.1124/dmd.117.078238
This article has not been copyedited and formatted. The final version may differ from this version.

was observed for *ABCB1/*MDR1, exhibiting comparable levels of those found in the primary hepatic model (Figure 2B). Relative expression levels of all other efflux transporters were lower to different extents in sandwich-cultures of different UHH donors compared to SCHH. Nevertheless, *ABCC2/*MRP2 and *SLC47A1/*MATE1 mRNA transcripts were readily detected and were present at levels to approximately one-third of that in SCHH.

Protein abundance of hepatic transporters was analyzed based on a bottom-up quantitative targeted absolute proteomics (QTAP) approach from digested plasma membrane fractions prepared from cultured cells from the same donor and seeding as used for mRNA expression analysis. The sample preparation method described herein has been modified based on optimized conditions reported previously (Masuda et al., 2008, 2009; Uchida et al., 2013). MPEX-PTS reagents combined with PMX and a tandem-combinatorial Lys-C/trypsin digestion increased MS/MS signals and quantification values of probe peptides, most likely due to enhanced membrane protein solubilization, digestion efficiency and peptide recovery. Intra-assay variability and validity of the bioanalytical quantification method was investigated in terms of linearity of calibration curves, precision and accuracy. For all target peptides analyzed, the correlation coefficients (r^2) were greater than 0.992 (Supplemental Table 4A). Inaccuracy was found below 20% and imprecision values were not greater than 15.4% based on the mean values of QC samples, derived from three to four transitions (Supplemental Table 4B, 4C), except for NTCP (inaccuracy of 20.4% in the middle amount quality control sample (MQC)). Representative SRM/MRM chromatograms for standard and QC samples as well as for samples derived from hepatic cell culture are provided in Supplemental Figure 2. The same proteomic methodology was applied to all samples derived from independent cultures of three different UHH and cPHH donors, respectively. Assuming that membrane purification, protein solubilization and digestion efficiency were similar for primary and

DMD Fast Forward. Published on December 6, 2017 as DOI: 10.1124/dmd.117.078238
This article has not been copyedited and formatted. The final version may differ from this version.

genetically modified upcyte hepatocytes samples, we compared quantified peptide levels as surrogate for the abundance of ten drug transporters and two membrane markers between the two hepatic in vitro systems evaluated.

In coincidence with the mRNA expression data (Table 2), considerable abundance of sinusoidal transporter proteins OATP2B1, OCT1 and NTCP could be demonstrated in samples derived from sandwich-cultures (Table 2), whereas quantified levels of OATP1B1 and OATP1B3 were found below LOQ or were not detected, respectively in any of the UHH donors evaluated, applying the conditions described herein. In contrast, OATP1B1 and OATP1B3 protein was quantifiable in SCHH from three donors with a mean of 11.0 ± 7.6 *f*mol/µg membrane protein and 2.01 ± 0.12 *f*mol/µg membrane protein (Supplemental Table 6), respectively, based on the selected peptides (Table 1, Supplemental Table 3) and the chosen sample preparation method. As depicted in Figure 2C, representing the average of quantification values derived from individual donors (Table 3), abundances of uptake transporter proteins and the commonly used basolateral membrane marker Na^+/K^+-ATPase were lower in SCUHH compared to levels of SCHH. OATP1B1 levels were considerably reduced in SCUHH and, unlike for SCHH (with levels ranging from 4.81 to 19.4 *f*mol/µg plasma membrane protein), no donor-related difference in protein abundance was observed. Average quantification levels of OATP2B1 and NTCP in SCUHH based on selected signature peptides (0.98 and 1.64 *f*mol/µg plasma membrane protein, respectively) were approximately one fifth and one third of the average amount quantified in SCHH, respectively (Supplemental Table 6). Abundance of OCT1 protein was determined based on the surrogate peptide LSPSFADLFR, in line with previous reports (Supplemental Table 3). Levels in SCUHH were 32-fold lower compared to quantified values in SCHH (Figure 2C; >76.4 ± 26.6 *f*mol/µg

DMD Fast Forward. Published on December 6, 2017 as DOI: 10.1124/dmd.117.078238
This article has not been copyedited and formatted. The final version may differ from this version.

plasma membrane protein), reflecting well the substantial difference observed at the gene level (Figure 2A).

All five hepato-canalicular expressed transporter proteins and the canalicular marker enzyme γ-GTP were detectable in samples from both hepatic systems. Quantified values for MDR1 derived from SCUHH (10.3 ± 5.6 *f*mol/μg plasma membrane protein) were in the same range as levels from SCHH (8.28 ± 2.97 *f*mol/μg plasma membrane protein). Furthermore, this finding is found consistent with gene expression data (Figure 2B). As shown in Figure 2D, average protein levels of MPR2, BCRP, BSEP and MATE1 based on selected signature peptides (Supplemental Table 3) were quantitatively lower, but within 10-fold of the amounts measured in SCHH. Interindividual protein levels of both hepatic models are summarized in Table 3.

Sinusoidal Drug Transporter Activities in Differentiated Cultures of UHH. Carrier-mediated uptake activities of UHH from the same three donors (151-03, 653-03, 10-03) were assessed by determining accumulation at 37°C (total uptake) and 4°C (passive diffusion) of rosuvastatin, taurocholate and MMP^+ as typical substrates for OATP1B1/B3/2B1 (Kitamura et al., 2008; Ho et al., 2006), NTCP (Trauner and Boyer, 2002) and OCT1 (Umehara et al., 2007), respectively. Uptake of radiolabeled substrates was reproducibly demonstrated in UHH post sandwich-culture (Table 4). The highest total uptake clearance (CL_{uptake}) in SCUHH was measured for MPP^+; whereas, a considerable low CL_{uptake} was observed for rosuvastatin. Furthermore, uptake rates were significantly higher at 37°C than at 4°C (except for rosuvastatin in cells from donor 653-03), indicating a substantial contribution of carrier-mediated transport to overall uptake of reference drugs evaluated (Supplemental Figure 4). CL_{uptake} of rosuvastatin, taurocholate and MPP^+ was lower in all SCUHH compared to that in

DMD Fast Forward. Published on December 6, 2017 as DOI: 10.1124/dmd.117.078238
This article has not been copyedited and formatted. The final version may differ from this version.

SCHH, the extent of which was donor-dependent (2.7- to 4.6-fold, 2.0- to 3.5-fold and 1.2- to 2.7-fold, respectively; Table 3). Nevertheless, percentages of transporter-mediated uptake (CL_{active}) for each substrate were generally in line with the extent of active contributions observed in SCHH. For rosuvastatin and taurocholate, interindividual variation in CL_{uptake} was similar between both hepatic models with a coefficient of variance (CV) between 28% and 34%; whereas the variation for MPP^+ was higher in SCUHH (37% CV) than in SCHH (5.5% CV).

To differentiate further between Na^+-dependent and OATP-mediated uptake activity in SCUHH, uptake rates of CCK-8 and pravastatin (as well as $E_2$17ßG, data not shown) were determined in SCUHH (donor 151-03) and SCHH at day 7. Uptake rates of CCK-8 and pravastatin were substantially lower in SCUHH compared to those in SCHH (Figure 3). There was no statistical difference between incubations at 37°C and 4°C, nor was the uptake inhibited by RIF SV, indicating a lack of carrier-mediated contributions to the overall uptake of these reference substrates in SCUHH. In contrast, uptake of rosuvastatin (Figure 3A) was substantially decreased to 28% of the control accumulation rate by RIF SV in SCUHH. In addition, RIF SV inhibited OATP-mediated uptake of rosuvastatin, CCK-8 and pravastatin by 64 ± 1.6%, 92 ± 2.2% and 61 ± 6.2 % in SCHH, respectively (Figure 3). In both hepatic culture models, differences in uptake rates of rosuvastatin and pravastatin observed between 4°C- and 37°C incubations containing RIF SV (1.6- to 2.1-fold and 1.1- to 2.3-fold, respectively), might be a result of altered fluidity of the plasma membrane at low temperature, restricting passive diffusion (Kimoto et al., 2011). Incomplete inhibition of active processes (Webborn et al., 2007) under the experimental conditions applied herein, might also explain this finding. Interestingly, cellular accumulation of CCK-8 was higher at 4°C compared to incubations at 37°C with RIF SV. We speculate that RIV SV displaced CCK-8 from its

DMD Fast Forward. Published on December 6, 2017 as DOI: 10.1124/dmd.117.078238
This article has not been copyedited and formatted. The final version may differ from this version.

temperature-dependent binding to cells or other proteins present in the incubation matrix, potentially leading to reduced accumulation rates observed. However, the estimated contribution of passive diffusion to total uptake of CCK-8 (21%; based on substrate accumulation determined at 4°C and depicted for SCHH in Figure 3) was found in line with reported values (28.6%, Kunze et al., 2014).

NTCP-mediated Uptake of Rosuvastatin in Upcyte Human Hepatocytes. Since OATP1B3 and OATP1B1 at the mRNA and protein level were not detected or only at very low levels in SCUHH using our methods, respectively (Tables 2 and 3), we investigated whether quantified peptide levels, considered as surrogate for NTCP and OATP2B1 protein abundance in the corresponding in vitro system, could be associated with the active uptake of rosuvastatin in SCUHH from different donors (Figure 4A). Being aware of the limited power resulting from the correlation analysis of only three UHH donors evaluated, NTCP and/or OATP2B1, rather than OATP1B1, seemed to be linked to the active uptake of rosuvastatin in SCUHH.

In a separate study, using different batches of cells (i.e. different seeding, which was not used for mRNA or quantitative proteomics analysis), the sodium (Na^+)-dependent uptake of rosuvastatin and taurocholate into SCHH and SCUHH under conditions of depleted extracellular Na^+ or in excess concentrations of taurocholate was investigated. Although uptake clearance of taurocholate (7.78 ± 1.55 µL/min/mg total protein) determined under control conditions (37°C, Na^+-containing buffer) was comparable to previous experiments (Table 4), uptake of rosuvastatin (2.46 ± 0.25 µL/min/mg total protein) was notably reduced in this particular batch of SCUHH. In SCHH, uptake clearance of both substrates (18.5 ± 3.1 and 16.1 ± 2.3 µL/min/mg total protein for taurocholate and rosuvastatin, respectively) were well in line with previous results (Table 4). In the absence of extracellular Na^+, hepatic uptake

DMD Fast Forward. Published on December 6, 2017 as DOI: 10.1124/dmd.117.078238
This article has not been copyedited and formatted. The final version may differ from this version.

of taurocholate was substantially decreased by 74% in both hepatic models (Figure 4B); whereas, the uptake of rosuvastatin uptake was only reduced by 27% in SCHH (Figure 4C). By contrast, Na^+-depletion caused a 46%-decrease of rosuvastatin uptake in SCUHH, suggesting a higher contribution of NTCP to the total hepatic uptake of this substrate in SCUHH compared to SCHH. In the presence of Na^+, an excess of unlabeled taurocholate significantly inhibited the uptake of radiolabeled taurocholate (Figure 4B) in SCHH (95% inhibition) as well as in SCUHH (85% inhibition). A marked inhibition was also observed in the hepatic uptake of rosuvastatin (Figure 4C), yet to a higher extent in SCHH (74%) than in SCUHH (55%).

DMD Fast Forward. Published on December 6, 2017 as DOI: 10.1124/dmd.117.078238
This article has not been copyedited and formatted. The final version may differ from this version.

DISCUSSION

Previously, UHH have been characterized regarding their hepatic phenotype and metabolic capabilities (Schaefer et al., 2016; Tolosa et al., 2016). However, sinusoidal and canalicular transport properties, as key attributes of differentiated hepatocytes, have so far not been described for UHH.

Results presented herein indicate that sinusoidal membrane transporters were poorly expressed or even undetectable (Table 2) in short-term cultures of UHH, in contrast to cPHH cultured for 4-6 hrs (data not shown; Kotani et al., 2011). Pursuant to this, uptake activities of OATP1B1/1B3/2B1, NTCP and OCT1 in short-term cultures of UHH were shown to be considerably lower compared to cPHH (unpublished data), according to cellular accumulation studies with reference substrates rosuvastatin (Figure 1, day 0), TCA and MPP^+ (data not shown). This finding is in agreement with data from others, who showed that cPHH maintain functional expression of uptake transporters at transporter- and/or lot-specific levels (Jigorel et al., 2005; Kotani et al., 2011; Kimoto et al., 2012). In addition to cryopreservation, which generally impacts uptake activity (Badolo et al., 2011), UHH additionally pass several subculture steps involving proteolytic dissociation prior to seeding at high cell density. This procedure likely contributes to the loss of functional cell surface proteins (Huang et al., 2010), which presumably impedes the use of suspended or short-term (i.e. 4-6 hrs) cultured UHH for uptake studies. However, according to our findings, UHH in 2D collagen/matrigel sandwich-configuration (SCUHH) recover from trypsinization, are able to restore membrane proteins and to exhibit considerable expression of OATP1B1, OATP2B1, NTCP and OCT1 after 5 to 7 days. This culture-time dependent increase in expression, notably the lack of functional uptake in short-term cultures, might also be attributed to the proliferation-inducing cytokine oncostatin M (OSM). It has been shown that OSM, similarly to interleukin-6, adversely

DMD Fast Forward. Published on December 6, 2017 as DOI: 10.1124/dmd.117.078238
This article has not been copyedited and formatted. The final version may differ from this version.

affects expression of sinusoidal SLC-transport proteins (Le Vee et al., 2011). Thus, the progressing uptake activity in sandwich-culture may be linked to OSM-withdrawal and consequently to an induced growth arrest and differentiation into mature hepatocyte-like cells with reported functional polarization (Levy et al., 2015). This hypothesis justifies the necessity of pre-culture periods at confluence prior to end-point-measurements, and is in line with previous results on cultivation time-dependent functionality of P450s in SCUHH (Schaefer et al. 2016). Therefore, investigations were performed after 7 or 14 days (donor 653-03) in sandwich-culture.

The expression of canalicular efflux pumps seemed to be preserved in SCUHH based on qRT-PCR and peptide-based LC-MS/MS analysis. MDR1/*ABCB1*, MATE1/*SLC47A1* and MRP2/*ABCC2* were notably expressed at donor-dependent levels (Figure 2B and D, Table 3), corresponding to a generally more stable expression of hepatic efflux transporters, as previously reported for PHH, HepaRG and HuH-7 cells (Yang et al., 2012; Le Vee et al., 2013; Jouan et al, 2017). Although expression of sinusoidal uptake transporters was considerably higher than that reported for hepatoma cell lines HuH-7 or HepG2 cells (Guo et al., 2010; Jouan et al., 2017), mRNA levels and quantified amounts of selected peptides were remarkably reduced in SCUHH compared to SCHH (Figure 2A and C). The most pronounced differences were observed for OATP1B1, and particularly for OATP1B3, coinciding with findings reported for differentiated HepaRG cells (mRNA levels were 7.0% and 0.6% of those in cPHH, respectively; Le Vee et al., 2013). Similar to OATP1B3 in HepaRG cells (Kotani et al, 2012), OATP1B3 mRNA and protein, based on the selected peptide, was virtually undetectable in SCUHH compared to SCHH at all time points evaluated. In addition, quantified OCT1 peptide levels, as well as transcript levels, were profoundly lower in SCUHH, contradicting the active uptake of MPP^+ demonstrated in SCUHH. Lacking evidence

DMD Fast Forward. Published on December 6, 2017 as DOI: 10.1124/dmd.117.078238
This article has not been copyedited and formatted. The final version may differ from this version.

of analytical/experimental effects, the OCT1 expression-activity discrepancy remains to be further investigated.

Variability of reported MS-based protein quantification values, likely biased by different methodological procedures applied and/or signature peptides selected, (Balogh et al., 2012; Badée et al., 2015; Peng et al., 2015, Harwood et al., 2016; Wegler et al., 2017), hampers direct comparison of absolute protein abundances among different laboratories. Considering this general limitation, quantified peptide levels in SCHH, measured under the chosen conditions, were yet within the range of published abundances, albeit OCT1 levels were found above reported values (Supplemental Table 6; Schaefer et al., 2012; Vilhede et al., 2015). Based on reported beneficial effects on solubilizing and digesting hydrophobic proteins by use of MPEX-PTS reagents and a tandem-combinational in-solution protocol (Masuda et al., 2008, 2009; Uchida et al., 2013) applied, we assume that observed discrepancies are rather linked to our sample preparation method, than to biological variability. In this context, quantitative protein values determined herein as supportive data together with mRNA levels, were intended to underpin differences observed in active uptake between the two hepatic models evaluated.

On a functional level, we primarily used rosuvastatin to assess overall OATP- and NTCP-mediated uptake properties of SCUHH and SCHH as suggested by Menochet et al. (2012). Uptake of rosuvastatin was saturable (Figure 1) and found appropriate to display interindividual variations observed at the gene and protein level. However, unlike the considerably different OATP1B1 abundances in SCHH (Table 3; Kimoto et al., 2012), OATP1B1/*SLCO1B1* expression showed no substantial interindividual variation in SCUHH, indicating that differences in CL_{uptake} observed between UHH donors could not be contributed solely to OATP1B1 activity. Given that rosuvastatin is a substrate of all three OATP isoforms

DMD Fast Forward. Published on December 6, 2017 as DOI: 10.1124/dmd.117.078238
This article has not been copyedited and formatted. The final version may differ from this version.

as well as NTCP (Ho et al., 2006; Bi et al., 2013) we attributed interindividual variations observed in the hepatic uptake of rosuvastatin by SCUHH to NTCP and/or OATP2B1. Indeed, besides the profound impact of the genetic variants *SLCO1B1*1B/*5/*15* on rosuvastatin pharmacokinetics (Giacomini et al., 2010; Yoshida et al., 2013; Patel et al., 2016), it has been shown, that the *NTCP*2* variant affects cellular accumulation of rosuvastatin compared to NTCP wildtype (Choi et al., 2011). In support of our assumption, and lacking information on the polymorphic forms of *SLCO* genes present in UHH donors evaluated, we first showed that rosuvastatin was significantly inhibited by RIF SV (Figure 3), a potent inhibitor of OATPs, but also of NTCP (Bi et al., 2013). By selecting additional OATP reference substrates, without a known profound contribution of OATP2B1 or NTCP, i.e. CCK-8 (OATP1B3/1B1; Ishiguro et al., 2006), pravastatin (OATP1B1; Hagenbuch and Gui, 2008), and $E_2$17ßG (mainly OATP1B1; Hirano et al., 2004) we could link reduced OATP1B1/1B3 activity in SCUHH to markedly poor expression observed for the respective genes. This observation may also relate to *SLCO1B1/1B3* genetic mutations, as discussed for HepaRG cells (Kotani et al., 2012). In contrast to the lack of correlation between OATP1B1/1B3 protein abundance and active uptake of rosuvastatin (CL_{active}) in SCUHH, a considerable quantitative protein expression-activity relationship was observed for NTCP-mediated uptake of taurocholate. CL_{active} of taurocholate was clearly attributed to NTCP in both hepatic models (Figure 4B), to a similar extent as that reported by Bi et al. (2013), confirming functional expression of NTCP in SCUHH. However, as hypothesized, the contribution of NTCP to Na^+-dependent uptake of rosuvastatin was found to be higher in SCUHH (46-55%), compared to our own (27%) and reported (28-35%) data for SCHH (Figure 4; Bi et al., 2013; Elsby et al., 2012; Kitamura et al., 2008; Ho et al., 2006). Furthermore, given that taurocholate is also a substrate of several OATPs (Kullak-Ublick et al., 2001; Takikawa, 2002), we assumed that the excess

DMD Fast Forward. Published on December 6, 2017 as DOI: 10.1124/dmd.117.078238
This article has not been copyedited and formatted. The final version may differ from this version.

of taurocholate also inhibited OATP-associated CL_{active} of rosuvastatin in SCHH (74% inhibition). By contrast, and potentially attributed to the lack of OATP1B1/1B3 expression and activity in SCUHH, taurocholate failed to increase the inhibitory effect associated with Na^+-depletion. Apart from NTCP, abundance of OATP2B1 was evident in SCUHH membrane fractions. Thus, along with the overlapping substrate specificity of OATP-isoforms (Kitamura et al., 2008), it appears reasonable to assume profound contribution of OATP2B1, in addition to NTCP, to the active uptake of rosuvastatin in SCUHH. Based on our results, we speculate that both SLC-transporters are able to compensate, at least to some extent, for low levels or absence of OATP1B1/1B3 activity in the uptake of xenobiotics with overlapping OATP/NTCP specificity, as discussed previously (Bi et al., 2013). Future, more comprehensive studies including additional reference drugs with diverse substrate specificity of NTCP and OATPs are required to strengthen this hypothesis.

In our efforts to evaluate the utility of SCUHH as in vitro tool to assess hepatic uptake-mediated clearance processes, the benchmark of SCHH, particularly regarding OATP1B1/1B3, was not met. Despite this limitation, SCUHH maintain expression of several canalicular efflux pumps and SLC uptake transporters at relevant levels. In addition, preliminary results (Supplemental Figure 5) indicated that expression of *SLCO1B1/1B3* and *SLCO2B1* in SCUHH can be modulated by change of culture medium, which may be related to the presence of dexamethasone and/or other activators of nuclear receptors (e.g. PXR or farnesoid X receptor (FXR)), and subsequently suggest the possibility to up-regulate OATP expression in SCUHH (Jigorel et al., 2006; Stieger and Hagenbuch, 2014). To what extent, remains to be investigated.

DMD Fast Forward. Published on December 6, 2017 as DOI: 10.1124/dmd.117.078238
This article has not been copyedited and formatted. The final version may differ from this version.

Applying the culture conditions described herein, SCUHH demonstrated NTCP-, OATP2B1- and OCT1-mediated uptake and thus might be considered as useful tool to elucidate compensatory and/or additional uptake pathways for OATP1B1/1B3 substrates.

DMD Fast Forward. Published on December 6, 2017 as DOI: 10.1124/dmd.117.078238
This article has not been copyedited and formatted. The final version may differ from this version.

ACKNOWLEDGEMENTS

We thank Asami Saito, Kaori Makino and Katsuya Kominami for technical support with sample quantitative proteomics, as well as Shinobu Suzuki for greatly supporting this collaborative work.

AUTHORSHIP CONTRIBUTIONS

Participated in research design: M. Schaefer and G. Schänzle

Conducted experiments: M. Schaefer and G. Morinaga

Performed data analysis: M. Schaefer and G. Morinaga

Wrote or contributed to the writing of the manuscript: M. Schaefer, A. Matsui, G. Schänzle, D. Bischoff, and R.D. Süssmuth

DMD Fast Forward. Published on December 6, 2017 as DOI: 10.1124/dmd.117.078238
This article has not been copyedited and formatted. The final version may differ from this version.

REFERENCES

Aninat C, Piton A, Glaise D, Le Charpentier T, Langouët S, Morel F, Guguen-Guillouzo C, and Guillouzo A (2006) Expression of cytochrome P450, conjugating enzymes and nuclear receptors in human hepatoma HepaRG cells. *Drug Metab Dispos* **34**: 75-83.

Badée J, Achour B, Rostami-Hodjegan A, and Galetin A (2015) Meta-analysis of expression of hepatic organic anion-transporting polypeptide (OATP) transporters in cellular systems relative to human liver tissue. *Drug Metab Dispos* **43**: 424-432.

Balogh LM, Kimoto E, Chupka J, Zhang H, and Yunrong L (2012) Membrane Protein Quantification by Peptide-Based Mass Spectrometry Approaches: Studies on the Organic Anion-Transporting Polypeptide Family. *J Proteomics Bioinform* **6**: 229-236.

Badolo L, Trancart MM, Gustavsson L, and Chesné C (2011) Effect of cryopreservation on the activity of OATP1B1/3 and OCT1 in isolated human hepatocytes. *Chem Biol Interact* **190**: 165-170.

Bi Y, Qui X, Rotter CJ, Kimoto E, Piotrowski M, Varma V, El-Kattan AF, and Lai, Y (2013) Quantitative assessment of the contribution of sodium-dependent taurocholate co-transporting polypeptide (NTCP) to the hepatic uptake of rosuvastatin, pitavastatin and fluvastatin. *Biopharm Drug Dispos* **34**: 452-461.

Choi MK, Shin HJ, Choi YL, Deng JW, Shin JG, and Song IS (2011) Differential effect of genetic variants of Na+-taurocholate co-transporting polypeptide (NTCP) and organic anion-transporting polypeptide 1B1 (OATP1B1) on the uptake of HMG-CoA reductase inhibitors. *Xenobiotica* **41:** 24-34.

Elsby R, Hilgendorf C, and Fenner K (2012) Understanding the critical disposition pathways of statins to assess drug-drug interaction risk during drug development: it's not just about OATP1B1. *Clin Pharmacol Ther* doi: 10.1038/clpt.2012.163.

Giacomini KM, Huang SM, Tweedie DJ, Benet LZ, Brouwer KLR, Chu X, Dahlin A, Evers R, Fischer V, Hillgren KM, Hoffmaster KA, Ishikawa T, Keppler D, Kim RB, Lee CA, Niemi M, Polli JW, Sugiyama Y, Swaan PW, Ware JA, Wright SH, Yee SW, Zamek-Gliszczynski MJ, and Zhang L (2010) Membrane transporters in drug development. *Nat Rev Drug Discov* **9**: 215-236.

Guo L, Dial S, Shi L, Branham W, Liu J, Fang JL, Green B, Deng H, Kaput J, and Ning B (2011) Similarities and differences in the expression of drug-metabolizing enzymes between human hepatic cell lines and primary human hepatocytes. *Drug Metab Dispos* **39**: 528-538.

Hagenbuch B, and Gui C (2008) Xenobiotic transporters of the human organic anion transporting polypetides (OATP) family. *Xenobiotica* **38**: 778-801.

Harwood MD, Achour B, Neuhoff S, Russell MR, Carlson GL, Warhurst G, and Rostami-Hodjegan A (2016) In vitro-In Vivo Extrapolation Scaling Factors for Intestinal P-glycoprotein and Breast Cancer Resistance Protein: Part I: A Cross-Laboratroy Comparison of Transporter Protein Abundances and Relative Expression Factors in Human Intestine and Caco-2 Cells. *Drug Metab Dispos* **44:** 297-307.

Hirano M, Maeda K, Shitara Y, and Sugiyama Y (2004) Contribution of OATP2 (OATP1B1) and OATP8 (OATP1B3) to the hepatic uptake of pitavastatin in humans. *J Pharmacol Exp Ther* **311**: 139-146.

Ho RH, Tirona RG, Leake BF, Glaeser H, Lee W, Lemke CJ, Wang Y, and Kim RB (2006) Drug and bile acid transporters in rosuvastatin hepatic uptake: function, expression, and pharmacogenetics. *Gastroenterology* **130**: 1793-1806.

Huang HL, Hsing HW, Lai TC, Chen YW, Lee TR, Chan HT, Lyu PC, Wu CL, Lu YC, Lin ST, Lin CW, Lai CH, Chang HT, Chou HC, Chan HL (2010) Trypsin-induced proteome alteration during cell subculture in mammalian cells. *J Biomed Sci* doi: 10.1186/1423-0127-17-36.

Ishiguro N, Maeda K, Kishimoto W, Saito A, Harada A, Ebner T, Roth W, Igarashi T, and Sugiyama Y (2006) Predominant contribution of OATP1B3 to the hepatic uptake of telmisartan, an angiotensin II antagonist, in humans. *Drug Metab Dispos* **34**: 1109-1115.

Ji C, Tschantz WR, Pfeifer ND, Ullah M, and Sadagopan N (2012) Development of a multiplex UPLC-MRM MS method for quantification of human membrane transport proteins OATP1B1, OATP1B3 and OATP2B1 in in vitro systems and tissues. *Anal Chim Acta* **717**: 67-76.

Jigorel E, Le Vee M, Boursiers-Neyret, Bertrand M, and Fardel O (2005) Functional expression of sinusoidal drug transporters in primary human and rat hepatocytes. *Drug Metab Dispos* **33**: 1418-1422.

Jigorel E, Le Vee M, Boursier-Neyret C, Permentier Y, and Fardel O (2006) Differential regulation of sinusoidal and canalicular hepatic drug transporter expression by xenobiotics activating drug-sensing receptors in primary human hepatocytes. *Drug Metab Dispos* **34**: 1756-1763.

Juoan E, Le Vée M, Denizot C, Permentier Y, and Fardel O (2016) Drug transporter expression and activity in human hepatoma HuH-7 cells. *Pharmaceutics* **9**: 3-14.

Kamiie J, Ohtsuki S, Iwase R, Ohmine K, Katsukara Y, Yanai K, Sekine Y, Uchida Y, Ito S, and Terasaki T (2008) Quantitative Atlas of Membrane Transporter Proteins: Development and Application of a Highly Sensitive Simultaneous LC/MS/MS Method Combined with Novel In-silico Peptide Selection Criteria. *Pharm Res* **25**: 1469-1483.

Kitamura S, Maeda K, Wang Y, and Sugiyama Y (2008) Involvement of multiple transporters in the hepatobiliary transport of rosuvastatin. *Drug Metab Dispos* **36**: 2014-2023.

Kimoto E, Chupka J, Xiao Y, Bi Y, and Duignan DB (2011) Characterization of digoxin uptake in sandwich-cultured human hepatocytes. *Drug Metab Dispos* **39**: 47-53.

Kimoto E, Yoshida K, Balogh LM, Bi Y, Maeda K, El-Kattan A, Sugiyama Y, and Lai Y (2012) Characterization of organic anion transporting polypeptide (OATP) expression and its functional contribution to the uptake of substrates in human hepatocytes. *Mol Pharm* **9**: 3535-3542.

Kotani N, Maeda K, Watanabe T, Hiramatsu M, Gong L, Bi Y, Takezawa H, Kusuhara H, and Sugiyama Y (2011) Culture period-dependent changes in the uptake of transporter substrates in sandwich-cultured rat and human hepatocytes. *Drug Metab Dispos* **39**: 1503-1510.

Kotani N, Maeda K, Debori Y, Camus S, Li R, Chesné C, and Sugiyama Y (2012) Expression and transport function of drug uptake transporters in differentiated HepaRG cells. *Mol Pharm* **9**: 3434-3441.

Kullak-Ublick GA, Ismair MG, Stieger B, Landmann L, Huber R, Pizzagalli F, Fattinger K, Meier P, and Hagenbuch B (2001) Organic anion-transporting polypeptide b (OATP-B) and its functional comparison with three other OAPTs of human liver. Gastroenterology 120: 525-533.

Kunze A, Huwyler J, Camenisch G, and Poller B (2014) Prediction of organic anion transporting polypeptide 1B1- and 1B3-mediated hepatic uptake of statins based on transporter protein expression and activity data. *Drug Metab Dispos* **42**: 1514-1521.

Le Vee M, jigorel E, Glaise D, Gripon P, Guguen-Guillouzo, and Fardel O (2006) Functional expression of sinusoidal and canalicular drug transporters in the differentiated human hepatoma HepaRG cell line. *Eur J Pharm Sci* **28**: 109-117.

Le Vee M, Jouan E, Stieger B, Lecureur V, and Fardel O (2011) Regulation of drug transporter expression by oncostatin m in human hepatocytes. Biochem Pharmacol **82**: 304-311.

Le Vee M, Noel G, Jouan E, Stieger B, and Fardel O (2013) polarized expression of drug transporters in differentiated human hepatoma HepaRG cells. *Toxicol In Vitro* **27**: 1979-1986.

Levy G, Bomze D, Heinz S, Ramachandran SD, Noerenberg A, Cohen M, Shibolet O, Sklan E, Branspenning J, and Nahmias Y (2015) Long-term culture and expansion of primary human hepatocytes. *Nat.Biotechnol* doi: 10.1038/nbt.3377.

Liu H, and Sahi J (2016) Role of hepatic drug transporters in drug development. *J Clin Pharmacol* **56**: S11-22.

Masuda T, Tomita M, and Ishihama Y (2008) Phase transfer surfactant-aided trypsin digestion for membrane proteome analysis. *J Proteome Res* **7:** 731-740.

Masuda T, Saito N, Tomita M, Ishihama Y (2009) Unbiased quantitation of Eschrichia coli membrane proteome using phase transfer surfactants. *Mol Cell Proteomics* **8:** 2770-2777.

Menochet K, Kenworthy KE, Houston JB, and Galetin A (2012) Use of mechanistic modeling to acess interindividual variability and interspecies differences in active uptake in human and rat hepatocytes. *Drug Metab Dispos* **40:** 1744-1756.

Nezasa K, Higaki K, Takeuchi M, Nakano M, and Koike M (2003) Uptake of rosuvastatin by isolated rat hepatocytes: comparison with pravastatin. *Xenobiotica* **33**: 379-388.

Ohtsuki S, Schaefer O, Kawakami H, Inoue T, Liehner S, Saito A, Ishiguro N, Kishimoto W, Ludwig-Schwellinger E, Ebner T, and Terasaki T (2012) Simultaneous absolute protein quantification of transporters cytochrome P450, and UDP-glucuronosyl-transferases as a novel approach for the characterization of individual human liver: comparison with mRNA levels and activities. *Drug Metab Dispos* **40**: 83-92.

Patel M, Taskar KS, and Zamek-Gliszczynski MJ (2016) Importance of hepatic transporters in clinical disposition of drugs and their metabolites. *J Clin Pharmacol* **56**: S23-39.

Peng K, Bacon J, Zheng M, Guo Y, and Wang MZ (2015) Ethnic Variability in the Expression of Hepatic Drug Transporters: Absolute Quantification by an Optimized Targeted Quantitative Proteomic Approach. *Drug Metab Dispos* **43**: 1045-1055.

Ramachandran SD, Vivarès, Klieber S, Hewitt NJ, Muenst B, Heinz S, Walles H, and Braspenning J (2015) Applicability of second-generation upcyte human hepatocytes for use in CYP inhibition and induction studies. Pharmacol Res Perspect doi: 10.1002/prp2.161.

Sakamoto A, Matsumaru T, Ishiguro N, Schaefer O, Ohtsuki S, Inoue T, Kawakami H, and Terasaki T (2011) Reliability and robustness of simultaneous absolute quantification of drug transporters, cytochrome P450 enzymes, and UDP-glucuronosyltransferases in human liver tissue by multiplexed MRM/selected reaction monitoring mode tandem mass spectrometry with nano-liquid chromatography. *J Pharm Sci* **100**: 4037-4043.

Schaefer M, Schaenzle G, Bischoff D, and Suessmuth RD (2016) Upcyte human hepatocytes: a potent in vitro tool for the prediction of hepatic clearance of metabolically stable compounds. *Drug Metab Dispos* **44**: 435-444.

Schaefer O, Ohtsuki S, Kawakami H, Inoue T, Liehner S, Saito A, Sakamoto A, Ishiguro N, Matsumaru T, Terasaki T, and Ebner T (2012) Absolute quantification and differential expression of drug transporters, cytochrome P450 enzymes, and UDP-glucuronosyl-transferases in cultured primary human hepatocytes. *Drug Metab Dispos* **40**: 93-103.

Stieger and Hagenbuch (2014) Organic anion transporting polypeptides. *Curr Top Membr* 73: 205-232.

Takikawa H (2002) Hepatobiliary transport of bile acids and organic anions. *J Hepatobiliary Pancreat Sci* **9**: 443-447.

Tolosa L, Gómez-Lechón MJ, López S, Guzmán C, Castell JV, Donato MT, Jover R (2016) Human upcyte hepatocytes: characterization of the hepatic phenotype and evaluation for acute and long-term hepatotoxicity routine testing. *Toxicol Sci* **152**: 214-229

Trauner M, and Boyer JL (2002) Bile salt transporters: molecular characterization, function and regulation. *Physiol Rev* **83**: 633-671.

Uchida Y, Ohtsuki S, Katsukura Y, Ikeda C, Suzuki T, Kamiie J, and Terasaki T (2011) Quantitative targeted absolute proteomics of human blood-brain barrier transporters and receptors. *J Neurochem* **117**: 333-345.

Uchida Y, Tachikawa M, Obuchi W, Hoshi Y, Tomioka Y, Ohtsuki S, and Terasaki T (2013) A study protocol for quantitative targeted absolute proteomics (QTAP) by LC-MS/MS: application for inter-strain differences in protein expression levels of transporters, receptors, claudin-5, and marker proteins at the blood–brain barrier in ddY, FVB, and C57BL/6J mice. *Fluids Barriers CNS* doi: 10.1186/2045-8118-10-21.

Umehara, KI, Iwatsubo T, Noguchi K, and Kamimura H (2007) Functional involvement of organic cation transporter1 (OCT1/Oct1) in the hepatic uptake of organic cations in humans and rats. *Xenobiotica* **37**: 818-831.

Vilhede A, Wiśniewski JR, Norén A, Karlgren M, and Artursson P (2015) Comparative Proteomic Analysis of Human Liver Tissue and Isolated Hepatocytes with a Focus on Proteins Determining Drug Exposure. *J Proteome Res* **14**: 3305-3314.

Wegler C, Gaugaz FZ, Andersson TB, Wiśniewski JR, Busch D, Gröer C, Oswald S, Weiss F, Hammer H, Joos TO, Poetz O, Achour B, Rostami-Hochaghan A, Van de Steeg E, Wortelboer HM, and Artursson P (2017) Variability in Mass Spectrometry-based Quantification of Clinically Relevant Drug Transporters and Drug Metabolizing Enzymes. *Mol Pharm* **14**: 3142-3151.

Webborn PJH, Parker AJ, Denton RL, and Riley RJ (2007) In vitro-in vivo extrapolation of hepatic clearance involving active uptake: theoretical and experimental aspects. *Xenobiotica* **37**: 1090-1109.

Yang Q, Doshi U, Li N, and Li AP (2012) Effects of Culture Duration on Gene Expression of P450 Isoforms, Uptake and Efflux Transporters in Primary Hepatocytes Cultured in the Absence and Presence of Interleukin-6: Implications for Experimental Design for the Evaluation of Down-regulatory Effects of Biotherapeutics. *Curr Drug Metab* **13**: 938-946.

Yoshida K, Maeda K, and Sugiyama Y (2013) Hepatic and intestinal drug transporters: prediction of pharmacokinetic effects caused by drug-drug interactions and genetic polymorphisms. *Annu Rev Pharmacol Toxicol* **53**: 581-612.

FOOTNOTES

This work was supported by Boehringer Ingelheim Pharma GmbH & Co. KG.

DMD Fast Forward. Published on December 6, 2017 as DOI: 10.1124/dmd.117.078238
This article has not been copyedited and formatted. The final version may differ from this version.

FIGURE LEGENDS

Figure 1. Culture-Time dependent Expression and Functional Uptake of Rosuvastatin in plated UHH

(A) Total hepatic uptake CL of [^{3}H]rosuvastatin ([^{3}H]RSV, 1 µM) was determined in cultured UHH (donor 151-03) at different time points (4-6 hrs, i.e. day 0 up to day 14). Each bar represents the mean ± S.D. of three to six separate measurements (n=3-6) from one to two independent experiments. Expression of OATP1B1/*SLCO1B1* was monitored by qRT-PCR using the same batches of cells. Levels of mRNA are depicted relative to endogenous control ß-actin as mean ± S.D. (n=6) of two individual experiments. Each sample for mRNA expression analysis represents a pool of at least three wells per time point (n≥3). Amplifications were performed in triplicate for each sample (n=3). (B) Time profiles of [^{3}H]rosuvastatin (1 µM) observed in SCUHH at days 3, 5, 7 and 10. Filled and open circles represent intracellular accumulation determined at 37°C and 4°C, respectively, for 1, 2, 5 and 10 minutes. Each data point is expressed as mean ± S.D. of three separate measurements from one batch of UHH (error bars are occasionally covered by the symbol). (C) Representative Michaelis-Menten plot of [^{3}H]rosuvastatin uptake at day 7 in SCUHH (donor 151-03). Uptake of [^{3}H]rosuvastatin was measured at concentrations from 0.05-25 µM at 4°C (dashed line; filled circles) and 37°C (solid line, filled circles), respectively; open circles represent carrier-mediated uptake. Uptake experiments were conducted for 5 minutes with the solid line representing the fitted curve. Each point is expressed as mean ± S.D. of three separate determinations (n=3).

DMD Fast Forward. Published on December 6, 2017 as DOI: 10.1124/dmd.117.078238
This article has not been copyedited and formatted. The final version may differ from this version.

Figure 2. Abundance of Hepatic Drug Transporters in Long-term Sandwich-Cultures of UHH and PHH

Transcript levels and abundance of sinusoidal (A, C) and canalicular (B, D) hepatic transporters were determined in sandwich-cultured upcyte hepatocytes (SCUHH) and primary hepatocytes (SCHH), respectively, at day 7 or day 14, representing culture days of maximum transport activity determined in SCUHH by uptake experiments with [^{3}H]rosuvastatin at different culture time points. Protein abundances (*f*mol/µg plasma membrane protein), based on selected probe peptides, were quantified from digested plasma membrane extractions representing the mean ± S.D. of individual levels derived from three different cultures/donors of SCUHH (n=3) or SCHH (n=3), respectively. Average mRNA levels for each hepatic cell model are expressed relative to endogenous control ß-actin as mean ± S.D. of four to nine (n=4-9) independent studies. The LOQ (as described in Materials and Methods) and ULQ, were used for calculation of the average protein levels. In case signature peptides were not quantifiable (NQ) by the QTAP method described herein, quantification values were set to zero for calculations of the average, consequently OATP1B3 levels are not depicted in the logarithmic scaling of the graph. Accordingly, cycle-threshold values of ≥36 or undetermined template amplifications were defined as below LOQ and set to zero for calculation of the average mRNA expression levels. Solid line represents conformity, dashed lines 10-fold error range, respectively. Values in brackets express percentages of mRNA or protein amounts relative to those in SCHH, respectively.

DMD Fast Forward. Published on December 6, 2017 as DOI: 10.1124/dmd.117.078238
This article has not been copyedited and formatted. The final version may differ from this version.

Figure 3. Transport Activities of Sinusoidal Uptake Transporters in SCUHH

Inhibitory effect of rifamycin SV (RIF SV) on OATP1B1/1B3- and NTCP-mediated uptake of (A) [^{3}H]rosuvastatin ([^{3}H]RSV), (B) [^{3}H]cholecystokinin-8 ([^{3}H]CCK-8) and (C) [^{3}H]pravastatin ([^{3}H]PRV) in SCUHH (donor 151-03), compared to primary human hepatocytes (SCHH, donor HC3-31) at culture day 7. Uptake of reference substrates was measured at 37°C (control condition) for up to 5 minutes in the presence or absence of 100 µM RIF SV and, in parallel at 4°C, respectively. Each value represents the mean ± S.D. of three to six (n=3-6) separate determinations from one to two independent studies (data for [^{3}H]RSV in donor HC3-31 from one experiment are depicted in Table 4, and used herein to calculate the mean over altogether two independent studies). Statistical significance between each incubation condition and the control as well as between incubations at 4°C and incubations in the presence of RIF SV were determined for each hepatic in vitro system by one-way ANOVA followed by Tukey's post hoc test (* p<0.05, ** p<0.01, *** p < 0.001, **** p < 0.0001).

DMD Fast Forward. Published on December 6, 2017 as DOI: 10.1124/dmd.117.078238
This article has not been copyedited and formatted. The final version may differ from this version.

Figure 4. Contribution of NTCP to Total Uptake of Rosuvastatin

Correlation analysis (A) between carrier-mediated uptake of [^{3}H]rosuvastatin ([^{3}H]RSV) and corresponding peptide levels as surrogate for OATP1B1 (crosses), OATP2B1 (squares) and NTCP (triangles) abundance determined in the same batches of sandwich-cultured UHH from three different donors, respectively. Significant correlation was not observed (Pearson correlation coefficients r = 0.847, p = 0.357 and r = 0.930, p = 0.240 for OATP2B1 and NTCP, respectively, compared to r = -0.452, p = 0.702 for OATP1B1). In a separate study, sodium (Na^+)-dependent uptake of [^{3}H]taurocholate ([^{3}H]TC; (B)) and [^{3}H]RSV (C) was determined at 37°C in Na^+-containing buffer (control condition), under Na^+-depletion and in the presence or absence of an excess concentration of taurocholate (1mM; TC) in SCUHH (donor 151-03) and SCHH (donor HC3-31) at day 7, respectively. Data points represent individual uptake rates from three to six separate determinations (n=3-6) per hepatic model, each plotted as mean ±-S.D. Statistical significance between each incubation condition and the control was determined for each hepatic in vitro system by one-way ANOVA followed by Tukey's post hoc test (* p<0.05, ** p<0.01, *** p < 0.001, **** p < 0.0001).

TABLES

Table 1: SRM/MRM Transitions of Peptides Probes for human OATP1B1 and OATP2B1

Protein	Target peptide	Peptide sequence	Ref.	Residue pos.[#]	Trans-membr. region[#]	MW (Da)	SRM/MRM transition (Q1/Q3)						DP (V)	CE (V)
							Parent Ion (m/z), z=2	Product Ions (m/z), z=1						
							Q1	Q3-1	Q3-2	Q3-3	Q3-4			
OATP1B1	OATP1B1_pep A	LNTVGIAK	1-6	402-409	402-425	814.6	408.3	588.4	388.3	487.3	702.4	29_{Q3-1}	81	
		LNTVGI*AK				821.6	411.8	595.4	395.3	494.3	709.4	25_{Q3-2}		
	OATP1B1_pep B	DQTANLTNQGK	9, 10	306-316	-	1188.6	595.3	547.3	774.4	946.5	332.2	23_{Q3-3}		
		DQTANLTNQGK*				1196.6	599.3	555.3	782.4	954.5	340.2	39_{Q3-4}		
OATP2B1	OATP2B1_pep A	VLLQTLR	1-5	363-369	367-388	841.6	421.8	630.4	517.3	389.3	743.5	24.7_{Q3-1}	80	
		VLLQTL*R				848.6	425.3	637.4	524.3	396.3	750.5	24.7_{Q3-2}		
	OATP2B1_pep B	YYNNDLLR	7-10	641-648	-	1069.5	535.8	744.4	299.1	136.1	327.1	24.7_{Q3-3}		
		YYNNDLLR*				1079.5	540.8	754.4	299.1	136.1	327.1	24.7_{Q3-4}		

CE = collision energy; DP = declustering potential; MW = molecular weight; Ref. = reference
Bold letters with an asterisk indicate stable isotope-labeled amino acid (AA) residues (^{13}C and ^{15}N)

[1)] Sakamoto et al., 2011; [2)] Uchida et al., 2011; [3)] Ohtsuki et al., 2012; [4)] Schaefer et al., 2012; [5)] Kunze et al., 2014; [6)] Wegler et al., 2017; [7)] Ji et al., 2012; [8)] Peng et al., 2015; [9)] Proteomedix Frontiers Inc./Tohoku University (unpublished data); [10)] present study

[#)] Position (start-end AA) of selected peptide within the targeted protein according to Uniprot database; www.uniprot.org/uniprot/Q9Y6l6 and www.uniprot.org/uniprot/Q94956

Table 2. Comparison of Drug Transporter mRNA Expression between Short-Term Cultures and 2D-Sandwich-Cultures of UHH

Transcript levels of hepatic transporters were determined by quantitative RT-PCR of total RNA preparations derived from plated cells, harvested 4-6 hours after plating (short-term culture) or post sandwich-culture (SCUHH). Expression levels of mRNA are depicted relative to endogenous control ß-actin with each sample representing a pool of 3 to 4 wells of cultured cells. Cycle-threshold values of ≥36 or undetermined template amplifications were defined as below limit of quantification (LOQ) and set to zero for calculation of the average (AVG). Data are expressed as mean ± S.E.M. of three separate determinations (n=3) in a single experiment. The AVG represents the mean ± S.D. of the different donors (n=3).

	Donor 151-03		Donor 653-03		Donor 10-03		AVG	
	Short-term Culture	SCUHH	Short-term Culture	SCUHH	Short-term Culture	SCUHH	Short-term Culture	SCUHH
	10³ fold ß-actin		*10³ fold ß-actin*		*10³ fold ß-actin*		*10³ fold ß-actin*	*10³ fold ß-actin*
OATP1B1	<LOQ	1.69 ± 0.27	<LOQ	1.11 ± 0.10	<LOQ	0.079 ± 0.002	0.00 ± 0.00	0.960 ± 0.816
OATP1B3	<LOQ	<LOQ	<LOQ	<LOQ	<LOQ	<LOQ	0.00 ± 0.00	0.00 ± 0.00
OATP2B1	<LOQ	10.8 ± 0.3	<LOQ	4.60 ± 0.51	0.723 ± 0.026	3.31 ± 0.31	0.241 ± 0.417	6.24 ± 4.00
OCT1	0.078 ± 0.002	9.83 ± 0.66	0.054 ± 0.003	2.78 ± 0.16	<LOQ	1.57 ± 0.14	0.044 ± 0.040	4.73 ± 4.46
NTCP	<LOQ	8.21 ± 0.18	<LOQ	3.76 ± 0.12	<LOQ	1.65 ± 0.06	0.00 ± 0.00	4.54 ± 3.35
MDR1	43.4 ± 2.2	52.0 ± 0.4	1.17 ± 0.08	24.5 ± 2.7	40.8 ± 2.9	43.2 ± 1.2	28.5 ± 23.7	39.9 ± 14.0
MRP2	37.5 ± 3.8	36.2 ± 1.4	2.72 ± 0.20	18.4 ± 1.6	55.8 ± 3.0	19.5 ± 0.6	32.0 ± 27.0	24.7 ± 10.0
BCRP	0.594 ± 0.078	0.273 ± 0.033	0.855 ± 0.052	0.704 ± 0.075	0.255 ± 0.029	0.104 ± 0.002	0.568 ± 0.301	0.360 ± 0.309
BSEP	35.2 ± 0.4	8.93 ± 0.09	1.94 ± 0.20	8.77 ± 0.40	8.05 ± 0.50	0.218 ± 0.034	15.1 ± 17.7	5.97 ± 4.98
MATE1	3.76 ± 0.63	6.90 ± 0.45	0.161 ± 0.017	5.65 ± 0.13	5.93 ± 0.30	4.19 ± 0.68	3.28 ± 2.91	5.58 ± 1.36

Table 3. Protein Abundance of Hepatic Drug Transporter in Sandwich-Cultures of UHH and PHH

	SCUHH			SCHH		
	Donor 151-03	Donor 653-03	Donor 10-03	Donor Hu1601	Donor HC3-31	Donor 371
	fmol/µg	*fmol/µg*	*fmol/µg*	*fmol/µg*	*fmol/µg*	*fmol/µg*
OATP1B1	<LOQ (0.338)	0.376 ± 0.063	<LOQ (0.338)	4.81 ± 0.25	19.4 ± 1.08	8.73 ± 0.74
OATP1B3	NQ	NQ	NQ	1.96 ± 0.73	1.93 ± 0.49	2.15 ± 0.49
OATP2B1	1.29 ± 0.13	0.849 ± 0.064	0.802 ± 0.133	4.51 ± 0.30	4.18 ± 0.34	4.70 ± 0.64
OCT1	1.79 ± 0.64	3.20 ± 0.57	2.28 ± 0.32	>ULQ (100)	81.7 ± 20.2	47.7 ± 13.0
NTCP	1.95 ± 0.82	1.19 ± 0.18	1.79 ± 0.47	5.11 ± 0.41	4.00 ± 0.60	4.12 ± 0.79
MDR1	7.28 ± 0.95	6.83 ± 0.71	16.8 ± 4.4	7.70 ± 0.87	11.5 ± 0.7	5.65 ± 0.59
MRP2	4.00 ± 0.21	1.43 ± 0.12	1.96 ± 0.08	19.7 ± 2.94	5.19 ± 0.28	3.67 ± 0.31
BCRP	1.63 ± 1.06	1.78 ± 0.40	1.81 ± 0.60	1.74 ± 0.37	3.02 ± 0.85	2.21 ± 0.53
BSEP	<LOQ (0.467)	0.570 ± 0.036	0.523 ± 0.049	3.22 ± 0.82	2.47 ± 0.14	3.15 ± 0.14
MATE1	<LOQ (0.334)	0.352 ± 0.066	<LOQ (0.334)	0.525 ± 0.138	0.614 ± 0.045	0.566 ± 0.078
Na/K-ATPase	6.45 ± 0.54	24.5 ± 1.8	22.7 ± 1.4	33.2 ± 3.52	23.6 ± 3.44	22.7 ± 1.68
γ-GTP	12.2 ± 2.3	15.9 ± 2.4	15.5 ± 0.6	42.8 ± 2.6	21.5 ± 0.7	32.2 ± 4.3

SCUHH = sandwich-cultured upcyte human hepatocytes
SCHH = sandwich-cultured human hepatocytes
LOQ = limit of quantification
ULQ = upper limit of quantification
NQ = not quantifiable

LOQ_{MATE1} = 0.334 *f*mol/µg plasma membrane protein
$LOQ_{OATP1B1}$ = 0.338 *f*mol/µg plasma membrane protein
LOQ_{BSEP} = 0.467 *f*mol/µg plasma membrane protein
ULQ_{OCT1} = 100 *f*mol/µg plasma membrane protein

Abundance of surrogate peptides for canalicular and sinusoidal transporter proteins were quantified from digested plasma membrane extractions derived from sandwich-cultured upcyte and primary hepatocytes (SCUHH and SCHH), respectively. Concentrations based on

selected signature peptides are given as total amount of plasma membrane protein (*f*mol/µg plasma membrane protein) and are expressed as mean ± S.E.M. of triplicates or quadruplicates (n=3-4 MRM transitions) of a single experiment. In case concentrations were found below 1 *f*mol/µg protein and the corresponding peak area of detected signals of at least two MRM transition were below 5000 counts, the limit of quantification (LOQ) was defined as described by Uchida et al. (2011). In brief, the protein level of a signature peptide equivalent to a peak area of 5000 counts was calculated based on the linear regression equations obtained from calibrations curves (determination coefficient $r^2 >$ 0.99, Supplemental Table 4). If signal peaks were not detectable for two or more MRM transitions of a signature peptide, the corresponding transporter protein was defined as not quantifiable (NQ), and was considered not to be present in the corresponding UHH culture, applying the QTAP method described herein.

DMD Fast Forward. Published on December 6, 2017 as DOI: 10.1124/dmd.117.078238
This article has not been copyedited and formatted. The final version may differ from this version.

Table 4: Comparison of Hepatic Uptake Activities between Long-term cultured Upcyte Hepatocytes and Primary Hepatocytes.

Uptake clearances (CL_{uptake}) of rosuvastatin (RSV), taurocholate (TC) and N-methyl-4-phenylpyridinium acetate (MPP^+) were determined from transport studies conducted for up to 5 minutes at 37°C on day 7 or day 14 (donor 653-03) post sandwich-culture using three different donors of upcyte human hepatocytes (UHH) and primary human hepatocytes (PHH), respectively. Passive clearance ($CL_{passive}$) was appraised from control incubations performed at 4°C. Data represent the mean ± S.D. of one to four separate experiments, each conducted with three separate determinations per condition (n=3). The average (AVG) specified in the table represents mean ± S.D. of three different donors.

	PHH/UHH Lot	CL_{uptake} (µL/min/mg protein)	$CL_{passive}$ (µL/min/mg protein)	Transporter-mediated uptake (%)
RSV	Hu1601	11.1 ± 0.6	1.48 ± 0.41	87
	371	19.2 ± 1.4	2.10 ± 0.54	89
	HC3-31	20.1 ± 1.1	4.16 ± 0.46	79
	AVG	**16.8 ± 5.0**	**2.58 ± 1.40**	
	151-03	6.26 ± 1.40[a]	0.868 ± 0.320[a]	86
	653-03	3.65 ± 0.25[b]	1.82 ± 0.24[b]	50
	10-03	4.37 ± 0.60	0.933 ± 0.130	79
	AVG	**4.76 ± 1.35**	**1.21 ± 0.53**	
TC	Hu1601	34.0 ± 4.7	0.442 ± 0.133	99
	371	49.2 ± 5.2	2.29 ± 1.34	95
	HC3-31	24.9 ± 0.9	2.30 ± 0.35	91
	AVG	**36.0 ± 12.3**	**1.68 ± 1.07**	
	151-03	11.7 ± 2.9[a]	1.02 ± 0.92[a]	94
	653-03	10.3 ± 2.1[b]	2.95 ± 1.40[b]	71
	10-03	18.1 ± 1.9	2.86 ± 0.51	84
	AVG	**13.4 ± 4.2**	**2.28 ± 1.09**	
MPP^+	Hu1601	32.9 ± 1.4	1.70 ± 0.18	95
	371	34.9 ± 2.6	0.131 ± 0.458	100
	HC3-31	36.7 ± 2.1	0.305 ± 0.292	99
	AVG	**34.8 ± 1.9**	**0.713 ± 0.859**	
	151-03	23.0 ± 5.9[b]	0.893 ± 0.794[b]	96
	653-03	12.6 ± 3.4[b]	1.92 ± 1.12[b]	85
	10-03	28.2 ± 4.0	0.175 ± 0.021	100
	AVG	**21.3 ± 7.9**	**1.00 ± 0.87**	

[a)] Data represent mean ± SD determined using all replicates of 3-4 independent experiments (n=9-12)

[b)] Data represent mean ± SD determined using all replicates of two independent experiments (n=6)

DMD Fast Forward. Published on December 6, 2017 as DOI: 10.1124/dmd.117.078238
This article has not been copyedited and formatted. The final version may differ from this version.

Figure 1:

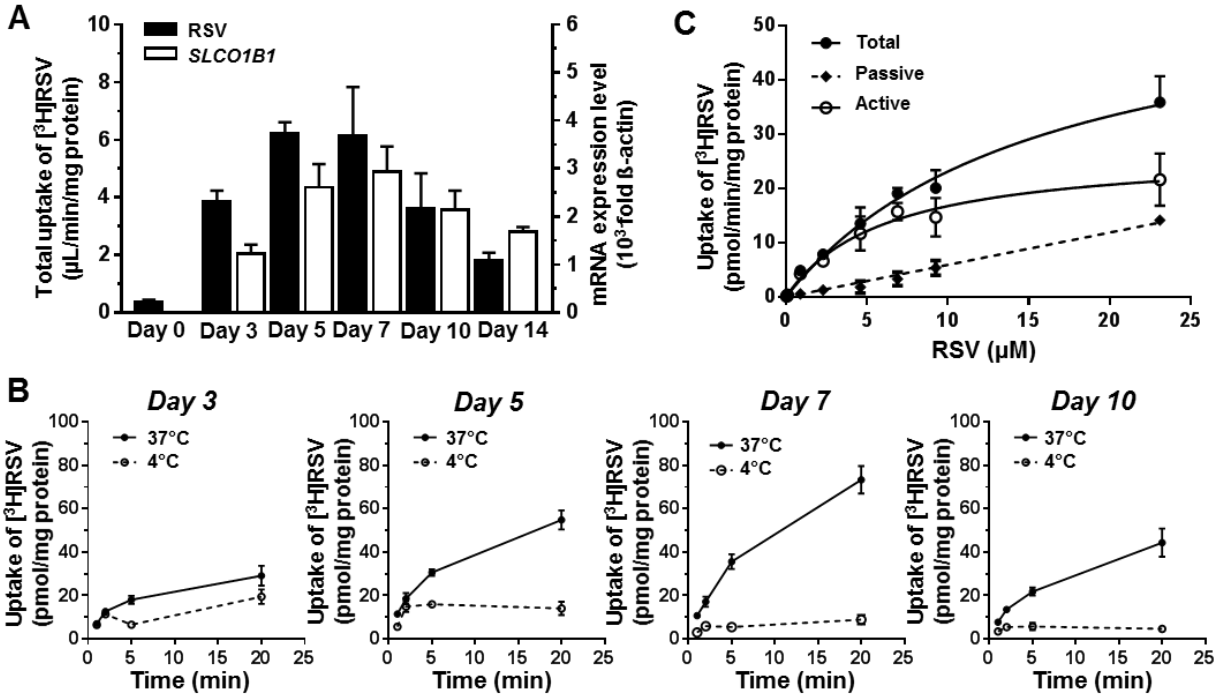

DMD Fast Forward. Published on December 6, 2017 as DOI: 10.1124/dmd.117.078238
This article has not been copyedited and formatted. The final version may differ from this version.

Figure 2:

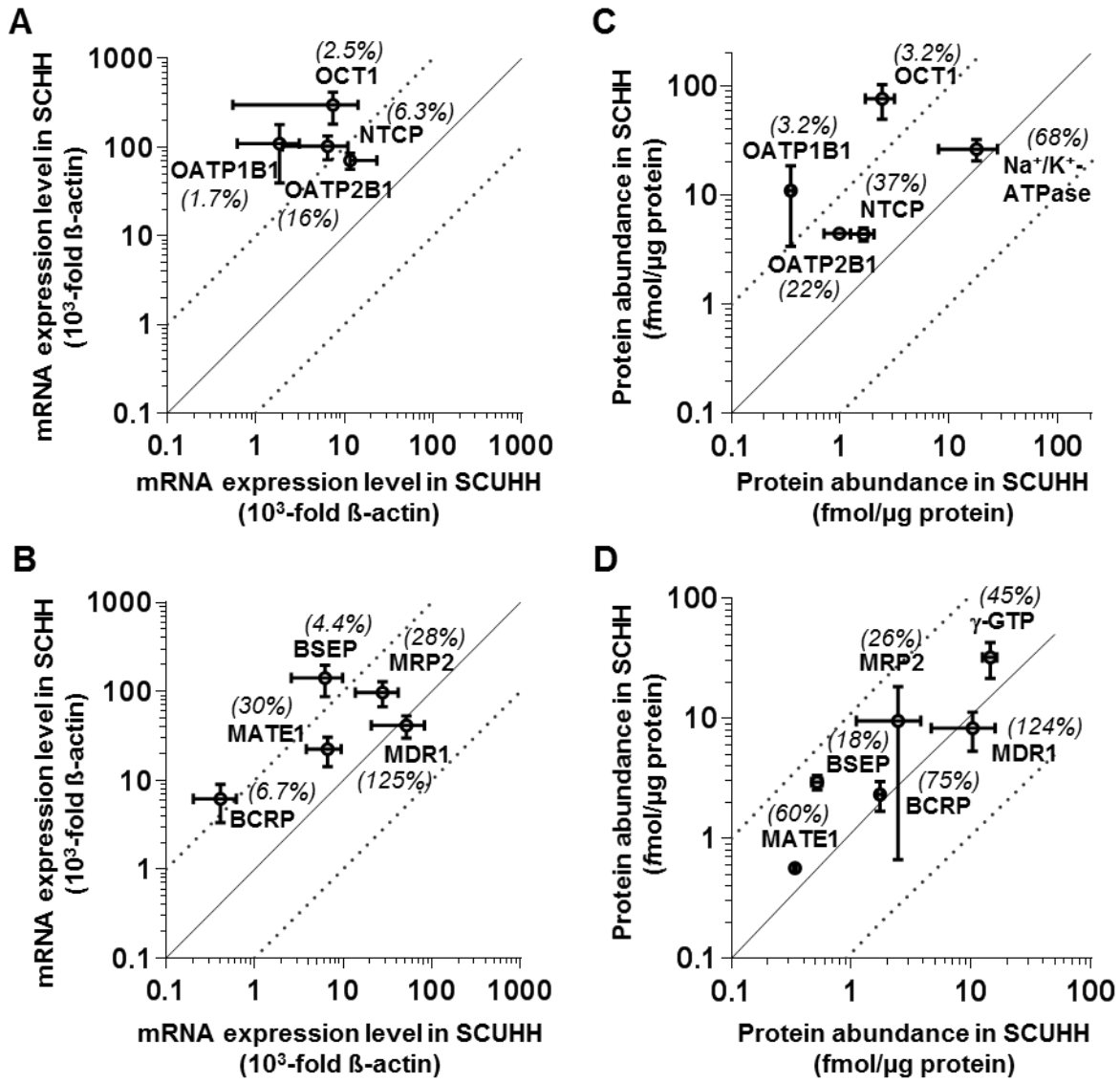

DMD Fast Forward. Published on December 6, 2017 as DOI: 10.1124/dmd.117.078238
This article has not been copyedited and formatted. The final version may differ from this version.

Figure 3:

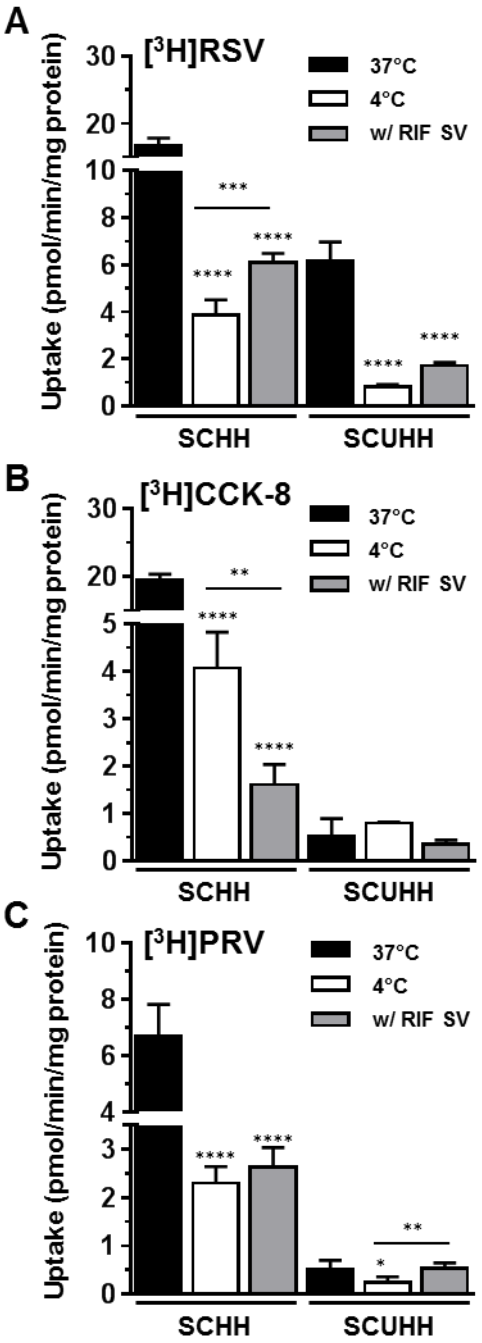

DMD Fast Forward. Published on December 6, 2017 as DOI: 10.1124/dmd.117.078238
This article has not been copyedited and formatted. The final version may differ from this version.

Figure 4: